NAVAL POSTGRADUATE SCHOOL
Monterey, California

THESIS

DETECTION OF MINES USING HYPERSPECTRAL ANALYSIS

by

Dimitrios Nikolaidis

June 1996

Thesis Advisor: David D. Cleary
Thesis Co-Advisor: Suntharalingam Gnanalingam

Approved for public release; distribution is unlimited.

REPORT DOCUMENTATION PAGE

Form Approved OMB No. 0704

1. AGENCY USE ONLY *(Leave blank)*	2. REPORT DATE June 1996	3. REPORT TYPE AND DATES COVERED Master's Thesis

4. TITLE AND SUBTITLE
DETECTION OF MINES USING HYPERSPECTRAL ANALYSIS

5. FUNDING NUMBERS

6. AUTHOR(S)
Nikolaidis, Dimitrios

7. PERFORMING ORGANIZATION NAME(S) AND ADDRESS(ES)
Naval Postgraduate School
Monterey CA 93943-5000

8. PERFORMING ORGANIZATION REPORT NUMBER

9. SPONSORING/MONITORING AGENCY NAME(S) AND ADDRESS(ES)

10. SPONSORING/MONITORING AGENCY REPORT NUMBER

11. SUPPLEMENTARY NOTES
The views expressed in this thesis are those of the author and do not reflect the official policy or position of the Department of Defense or the U.S. Government.

12a. DISTRIBUTION/AVAILABILITY STATEMENT
Approved for public release; distribution unlimited

12b. DISTRIBUTION CODE

13. ABSTRACT *(maximum 200 words)*

This study focuses on the development of computer algorithms that can be used for automatic mine detection using hyperspectral imagery. These algorithms perform a pixel-by-pixel comparison of the scene spectra with the spectrum of a mine. The goal is to assign to every pixel a scale factor which gives the relative probability of finding a mine. Algorithms were tested on simulated data taken from the NPS Middle Ultraviolet Spectrograph (MUSTANG). Three computer methods are tested and relative results were compared. This analysis suggests that the potential exists to use these methods in military applications. The ability to identify features in an image based solely on their spectral signature provides a new dimension to imagery interpretation.

14. SUBJECT TERMS
Strategic planning, computer software, Graphcis COPE, Expert Choice, cognitive mapping, Analytic Hierarchy Process,

15. NUMBER OF PAGES
64

16. PRICE CODE

17. SECURITY CLASSIFICATION OF REPORT	18. SECURITY CLASSIFICATION OF THIS PAGE	19. SECURITY CLASSIFICATION OF ABSTRACT	20. LIMITATION OF ABSTRACT
Unclassified	Unclassified	Unclassified	UL

NSN 7540-01-280-5500

Standard Form 298 (Rev. 2-89)
Prescribed by ANSI Std. 239-18

Approved for public release; distribution is unlimited.

DETECTION OF MINES USING HYPERSPECTRAL ANALYSIS

Dimitrios Nikolaidis
Lieutenant, Hellenic Navy
B.S., Hellenic Naval Academy, 1987

Submitted in partial fulfillment
of the requirements for the degree of

MASTER OF SCIENCE IN APPLIED PHYSICS

from the

NAVAL POSTGRADUATE SCHOOL
June 1996

Author: _____
Dimitrios Nikolaidis

Approved by: _____
David D. Cleary, Thesis Advisor

_____
Suntharalingam Gnanalingam, Thesis Co-Advisor

_____
William B. Colson, Chairman, Department of Physics

ABSTRACT

This study focuses on the development of computer algorithms that can be used for automatic mine detection using hyperspectral imagery. These algorithms perform a pixel-by-pixel comparison of the scene spectra with the spectrum of a mine. The goal is to assign to every pixel a scale factor which gives the relative probability of finding a mine. Algorithms were tested on simulated data taken from the NPS Middle Ultraviolet Spectrograph (MUSTANG). Three computer methods are tested and relative results were compared. This analysis suggests that the potential exists to use these methods in military applications. The ability to identify features in an image based solely on their spectral signature provides a new dimension to imagery interpretation.

TABLE OF CONTENTS

ACKNOWLEDGMENTS

This thesis could not have been completed without exceptional patience of my thesis advisor whom I also consider my friend, David D. Cleary, Ph.D.

Finally, and most importantly, my deepest thanks and appreciation to my family - Peggy and Chrysanthi - for their patience and understanding during the many months it took to put everything together. Their support was crucial to the completion of this work and they deserve the highest recognition for encouraging me as I completed my thesis.

I. INTRODUCTION

A mine, in a munitions sense, is "a receptacle filled with explosive, placed in or on the ground for destroying enemy personnel or material, or moored beneath or floating on or near the surface of water for destroying or impeding enemy ships" [Ref. 1: p. 205]. With the above definition as a reference, we can classify mines according to their intended target or the enviroment for which they are designed; anti-tank mines, anti-personnel mines, beach mines and so on. They can also be classified by their trigger mechanism, for example: acoustic mines, pressure mines. Mines are not only characterized by their design, but also by the method they are detected and handled.

Based on lessons learned from the past, the most important issue regarding mines is their efficient detection and safe avoidance. Several methods have been implemented to detect and destroy mines. Some of them involve primitive but effective techniques. Technology is expected to play an increasing role in future mine detection techniques.

When minefields are cleared by hand, detection is either by hand, prodding with a prodder or bayonet, or by mine detector. Mine prodding is slow but relatively safe, although a number of fuzes can be employed that are sensitive to metallic prodders, or actuate on movement of the mine. Current mine detectors work on a principle of low frequency (LF) induction and electrical

impedance, and therefore only pick up metallic mines or mines with a high proportion of metallic components. This type of detector is useless against fully non-metallic mines, and indeed can actuate some kinds of influence fuzes.

For the reasons above and keeping in mind the importance of saving time and lives in an anti-mine warfare theater, it is worth exploring the possibility of automating mine detection. There is a small but important class of mines called surface mines that lie exposed on the ground. One could automate the detection of these mines over a wide area using hyperspectral imaging. Hyperspectral imaging is an extension of multispectral imaging where instead of several spectral bands per pixel there are several hundred spectral channels per pixel. Because all materials have unique spectral signatures, one could detect a mine from its unique spectrum in a hyperspectral image. One such method would use hyperspectral imagery to identify mine signatures (signals). Every material has a specific spectral pattern that distinguishes it from other materials. As an example of spectral identification consider Figures 1.1 and 1.2 which show the spectra of a piece of white paper and typical beach-sand, respectively. Both of these materials were illuminated by an incandescent lamp. One can compare the two graphs and easily distinguish one from the other. A computer algorithm could be developed to make this distinction as well. While in general the problem can be quite complicated, in principle one can distinguish a mine from its surroundings using this technique.

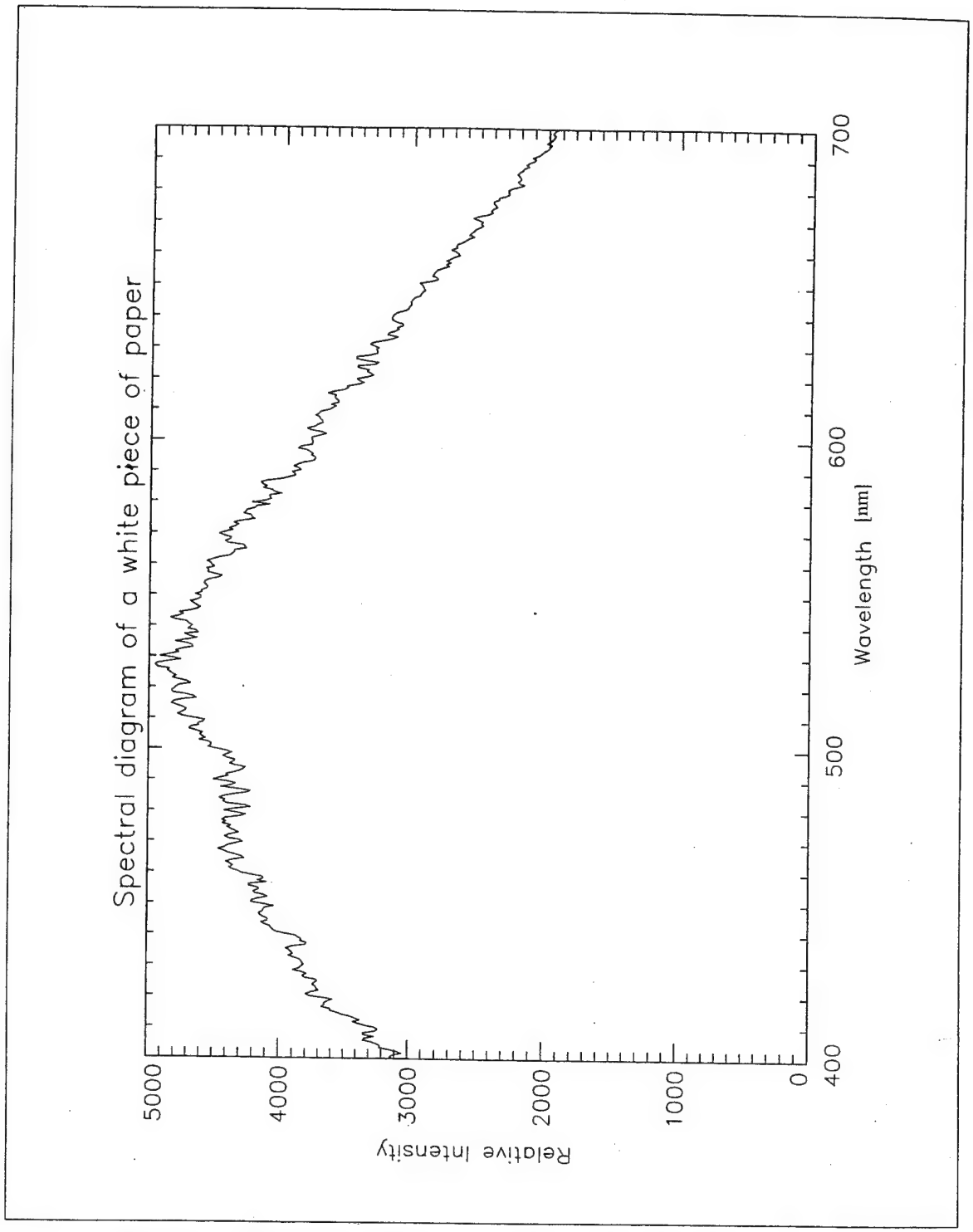

Figure 1.1: Spectral diagram of a white piece of paper

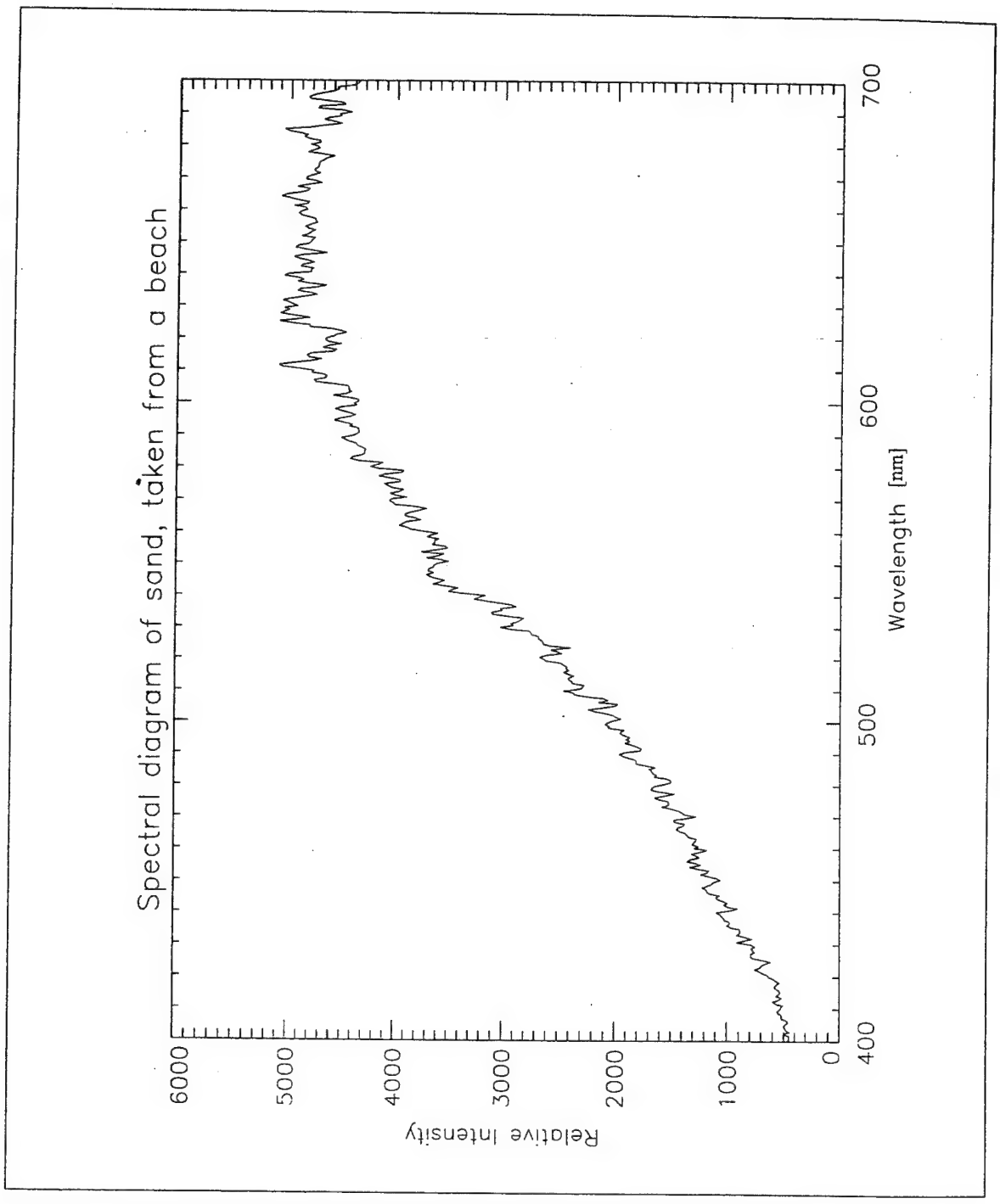

Figure 1.2: Spectral diagram of sand, taken from a beach

A. THESIS OBJECTIVES

This thesis focuses on the development of computer algorithms that can be used for mine detection. Using hyperspectral imagery these algorithms would perform a pixel-by-pixel spectral analysis. The goal is to assign to every pixel a scale factor which gives the relative probability of finding a mine. Algorithms were tested on simulated data taken from the NPS Middle Ultraviolet Spectrograph (MUSTANG). Three methods were tested and relative results were compared.

B. THESIS OUTLINE

This thesis is separated into four chapters and one appendix. Chapter II gives general background information on spectral and remote sensing issues. A basic explanation of radiometric quantities is also outlined in this section. Chapter III presents a complete description of the three search algorithms. Chapter IV presents a summary of findings and suggestions for future study. The appendix presents an overview and a brief description of the used programs/listings.

II. THEORETICAL BACKGROUND

Before describing the search algorithms, it is important to understand the scientific basis that supports the current study. This chapter introduces and explains the physical concepts behind the science of spectral images and remote sensing.

A. REMOTE SENSING

The physical phenomenon that makes remote sensing possible is electromagnetic radiation. By quantitatively measuring the properties of the electromagnetic radiation arriving at a sensor (like a spectrometer), scientists can gain an abundance of information about the earth's surface or atmosphere. The intensity of electromagnetic radiation collected by a remote sensor is controlled by the intensity of the source of illumination, the atmosphere through which it propagates, and the reflecting surface from which it is received. How electromagnetic radiation from the source is changed by the reflecting surface and the atmosphere provides the information sought by remote sensing users. Therefore, understanding the properties of this radiation is necessary for analysis of remotely sensed data. [Ref. 2 : p.41]

1. Refraction and reflection of electromagnetic waves

Energy is carried from its source by electromagnetic radiation, either directly through free space or indirectly by reflection and reradiation [Ref. 2 : p.37]. This radiative energy moves through space as electromagnetic waves. These waves are propagated by alternating electric and magnetic field components, lying on two planes that are mutually orthogonal, as can be seen in Figure 2.1. [Ref. 3 : p.843-854]

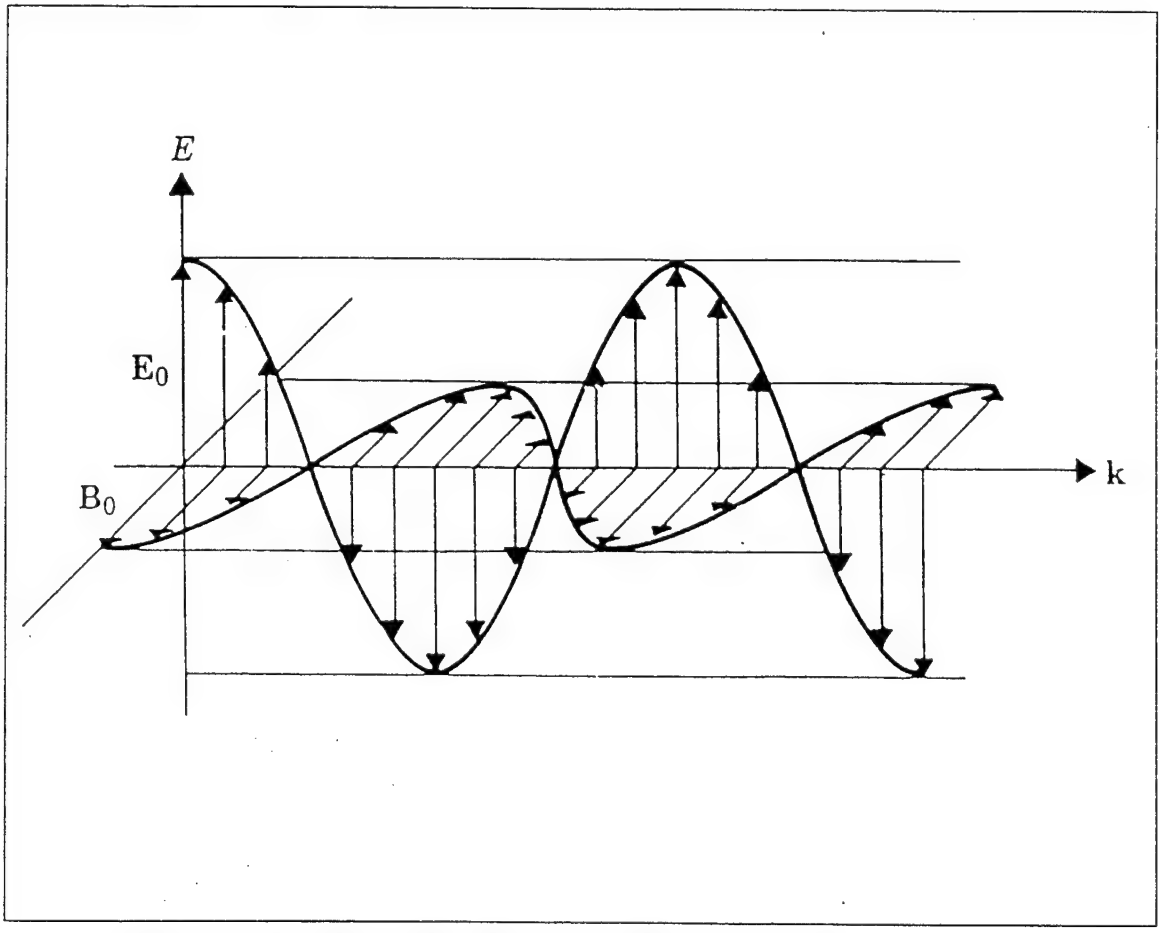

Figure 2.1: Electromagnetic Wave [Ref. 4 : p.47]

Because of its wave properties, electromagnetic radiation has a wavelength and frequency. The relationship between wavelength, λ, frequency, ν and the velocity of light in a vacuum, c, is given by:

$$\lambda = \frac{c}{\nu}$$

When an electromagnetic wave penetrates matter, its velocity changes according to the index of refraction of the medium. This refractive index is the ratio of the velocity of light in a vacuum to the velocity of light in the medium. Because the frequency remains constant, the wavelength changes upon interaction with a medium. This causes a bending or refraction of the wave.

Snell's Law defines the extent of the refraction as

$$n_1 \cdot \sin\theta_1 = n_2 \cdot \sin\theta_2 ,$$

where n_1 is the index of refraction for material 1, θ_1, is the angle of the incident ray from the normal, n_2 is the refractive index for material 2, and $\theta_2$is the angle of the refracted ray from the normal.

If the medium is isotropic, the incident ray, the normal to the surface, the reflected ray, and the refracted ray all lie in the same plane, as is shown in Figure 2.2.

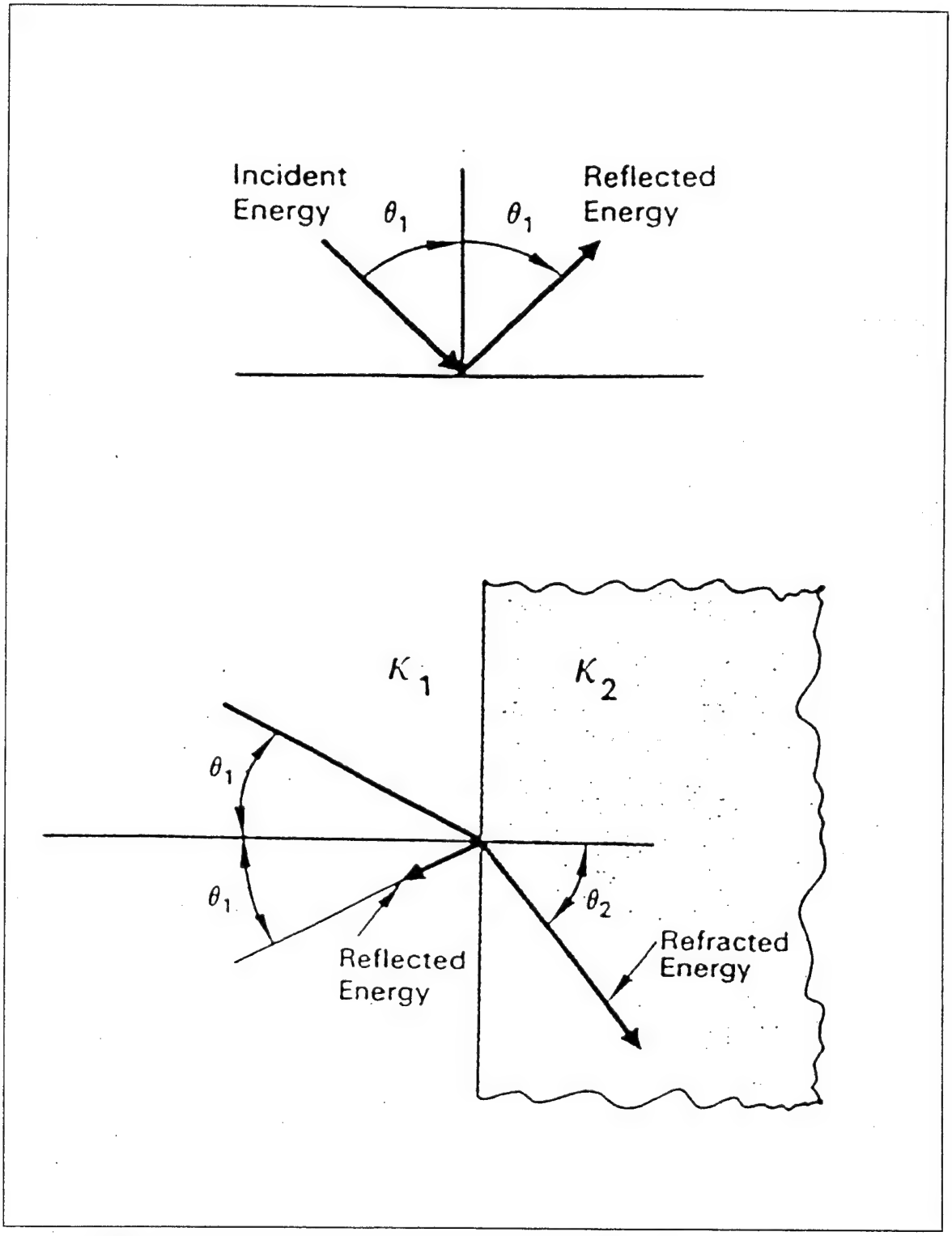

Figure 2.2: Refraction of light energy [Ref.6 : p.82]

2. Electromagnetic Spectrum

Electromagnetic radiation naturally provides a fast communicatons link between a sensor and its remotely located target. The various regions of the electromagnetic spectrum between 10^3 Hz to 10^{18} Hz are shown in Figure 2.3.

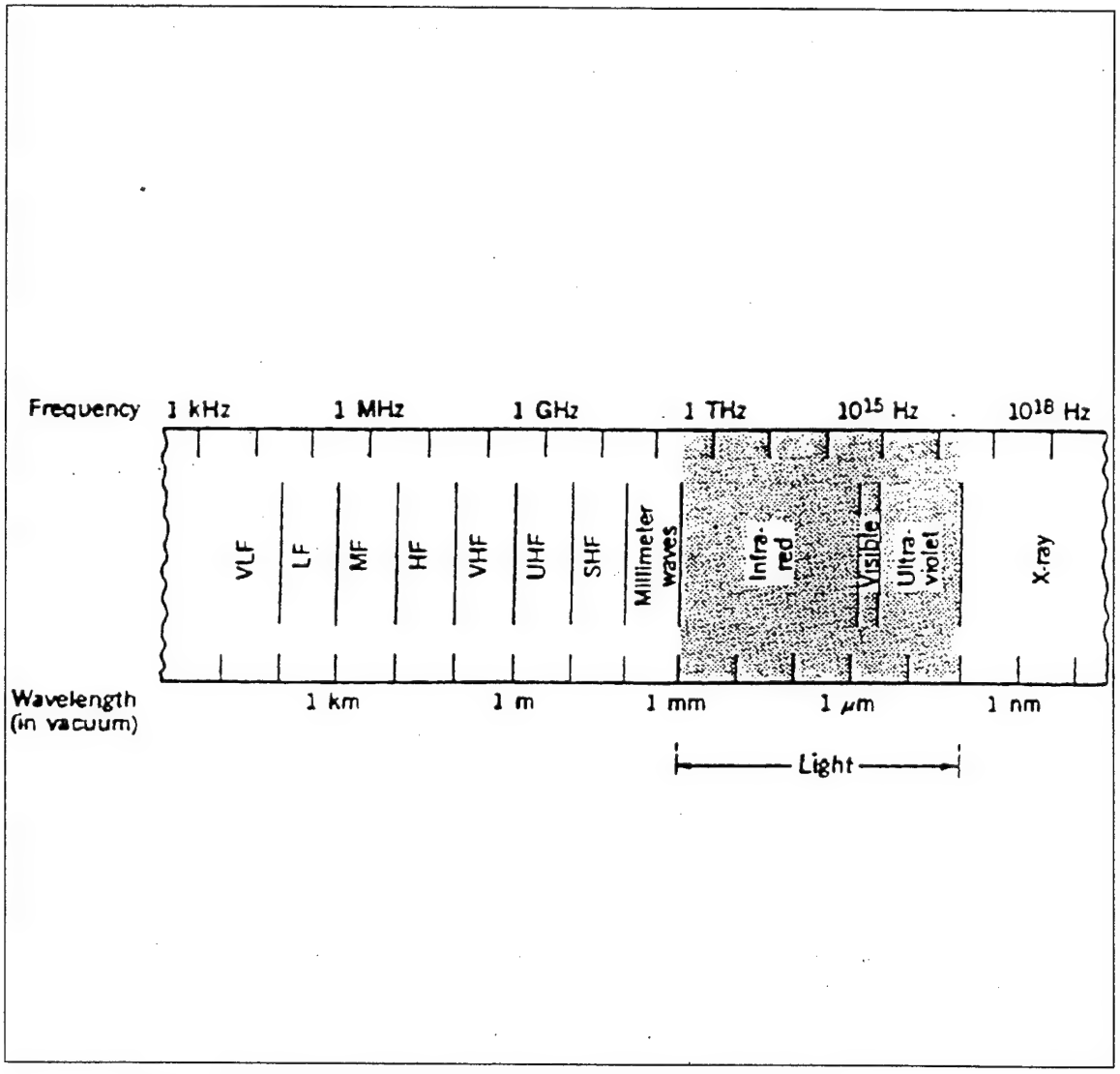

Figure 2.3: Electromagnetic Spectrum [Ref. 8 : p.34]

The most useful wavelengths for remote sensing are the optical wavelengths which extend from 0.30 to 15 microns. The electromagnetic energy in this wavelength range can be reflected or refracted by mirrors or lenses built to precision tolerance for remote sensing systems. [Ref. 9 : p.33]

3. Geometry of Remote Sensing

Fundamental to the measurement of electromagnetic radiation by a remote sensor is the concept of solid angle geometry. Because the distances between radiation sources and sensors are finite and radiation does not actually move in parallel rays, electromagnetic energy diverges radially from its source. The mathematical representation of this reality is accomplished with solid angles. The basic idea is that if a small portion of a sphere with radius, R, encloses a cone, the solid angle of the cone is equal to the area of the sphere enclosed by the cone divided by R^2. This is shown schematically in Figure 2.4. The unit of a solid angle is the steradian. Since the surface area of a sphere is $4\pi R^2$, a sphere contains 4π steradians of solid angle. Consider a remote sensing system a distance away from an energy-emitting target. The system's sensor is a flat plate of a particular area. This area can be used to calculate the solid angle of radiated energy even though the area of the flat plate is not exactly the same as the area of a sphere of the same radius. As long as the distance between the sensor and target is large compared to the size of the plate, this calculation is reasonably valid.

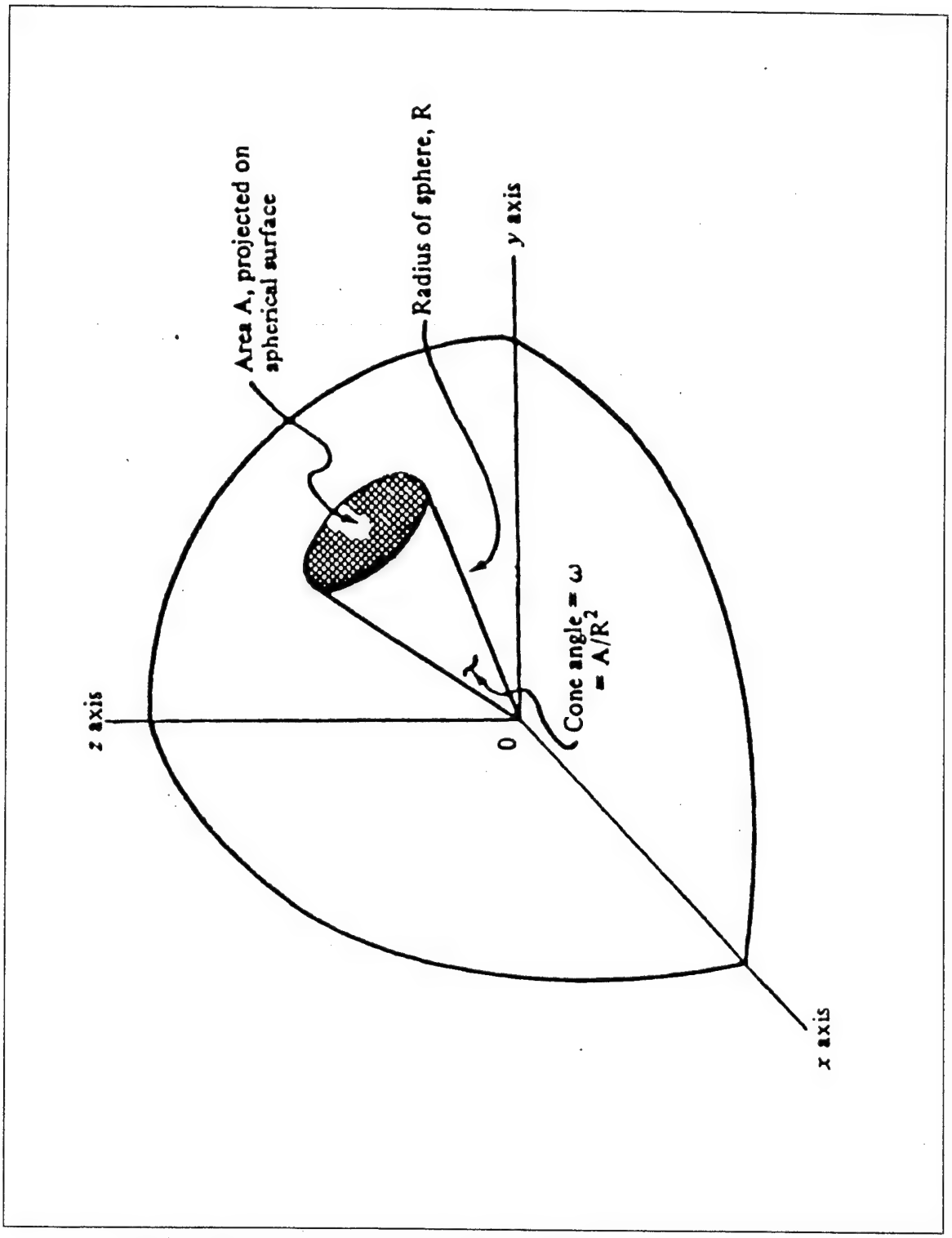

Figure 2.4: The concept of a Solid Angle

4. Radiative Transfer Quantities

Before explaining the concepts of radiative transfer, it is necessary to first define the radiometric quantities associated with remote sensing. Radiance is the radiant energy per unit time per unit solid angle coming from a specific direction , and which passes through a unit area perpendicular to that direction. This is shown schematically in Figure 2.5. The symbol for radiance is L, and its dimensions are Watts per meter squared per steradian (W/m^2-sr).

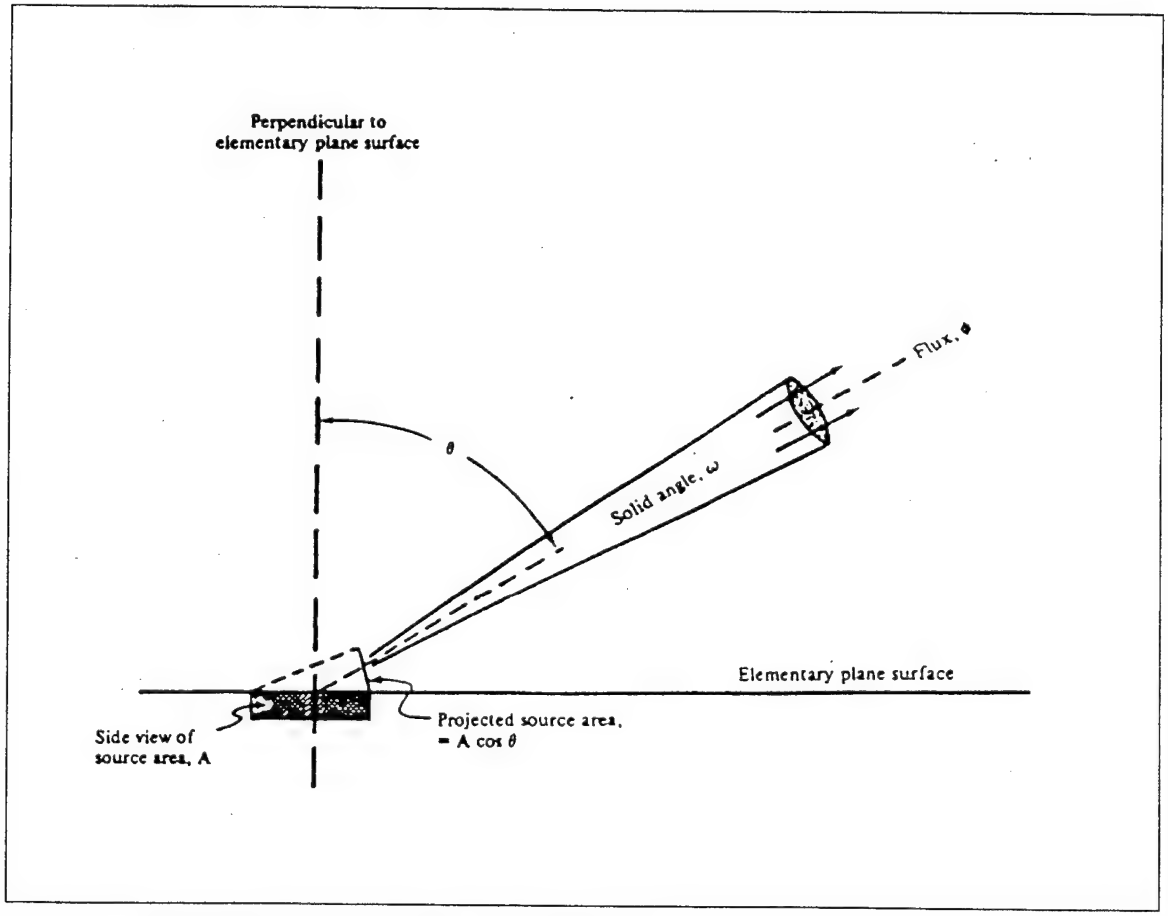

Figure 2.5: The concept of Radiance

Another important quantity is irradiance or radiant flux density, which is the total flux of photons flowing into a particular point per unit area from all directions, as is shown in Figure 2.6. The radiant flux density leaving a surface is called exitance. This quantity is important in remote sensing because knowing how different surfaces emit photons can help derive information about a target (mine) when its radiance is measured at a sensor.

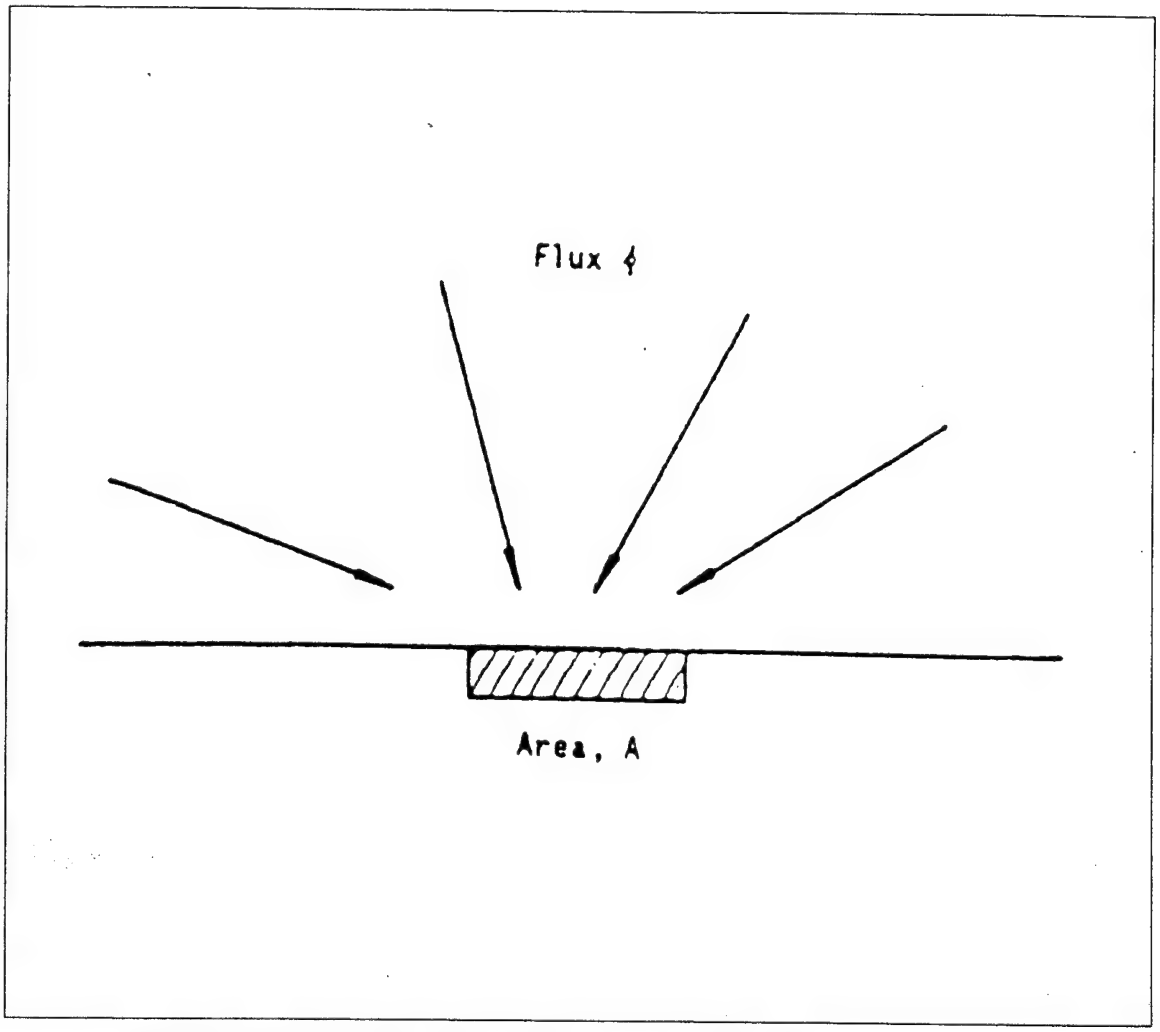

Figure 2.6: The concept of Radiant Flux Density

B. SPECTRAL CHARACTERISTICS

An important radiometric quantity, especially in imaging spectroscopy, is spectral reflectance. Spectral reflectance is the reflectance of a material as a function of wavelength and is determined by the manner in which radiation interacts with the earth's surface [Ref. 9 : p.38]. In order to identify ground features, it is essential to know their spectral reflectances.

For the visible and near IR regions, the spectral radiance at a sensor is the solar radiation reflected by a place on the earth's surface and modified by the atmosphere, as is shown in Figure 2.7. By measuring this radiance, and knowing the atmospheric spectral transmittance, the spectral reflectance of the surface can be derived. Reflectance of a feature or target on the earth's surface is the ratio of the measured irradiance and the atmospherically altered solar irradiance. A spectrum of reflectance values for a target can be created by measuring the radiance over a range of wavelengths. This spectrum of reflectances is commonly referred to as the spectral signature of the target (mine). The ability to identify targets on the earth's surface through analysis of spectral signatures is the objective of imaging spectroscopy.

Under ideal circumstances, spectral signatures could be used to accurately detect and locate targets on the earth's surface by analyzing hyperspectral data, because such data have high spectral resolution. However, spectral signatures are not single valued or completely independent of other

factors. A target's moisture content, background, and illuminating and viewing geometries, among other factors, can alter its observed reflectance spectrum. Therefore, spectral analysis must be accompanied with spatial information in order to draw accurate conclusions about targets on the earth's surface. [Ref. 7 : p.97]

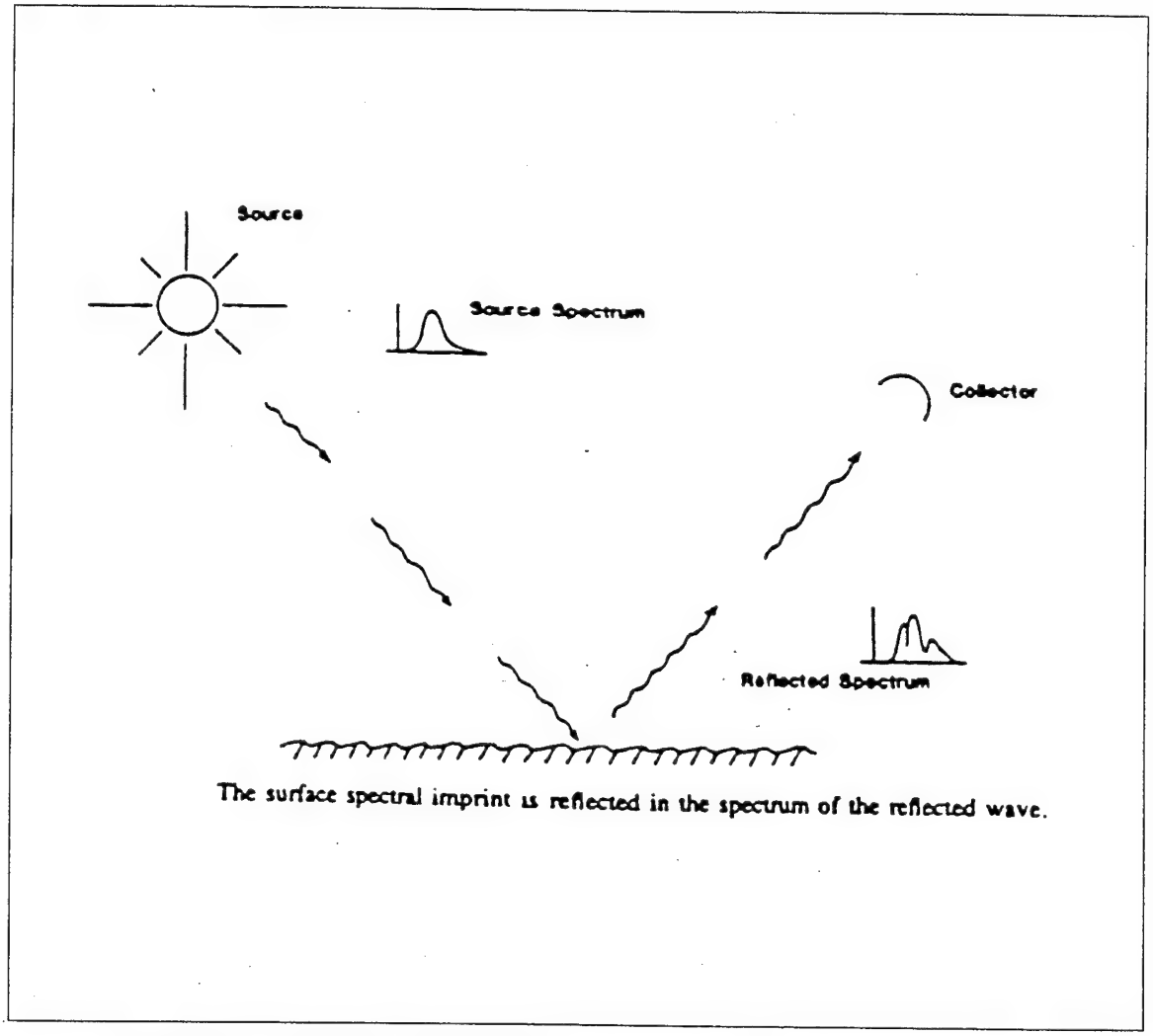

Figure 2.7: Spectral Reflectance

III. DESCRIPTION OF SEARCH ALGORITHMS

Before presenting the description of the search algorithms, we require the following definitions :

- Observations or test data are data taken from previous experimental observations.
- Reference spectrum or spectrum of a mine is the known spectrum from several mine types.
- Background spectrum is the spectrum of the natural enviroment like sea, beach, ground, etc.

Because actual observations of a scene containing mines were not available, each search algorithm was tested on simulated observations. These simulated observations or so-called test data consist of spectra containing both reference spectra and background spectra. The test data are taken from atmospheric observations using the NPS Middle Ultraviolet Spectrograph (MUSTANG). Because the spectra of the atmospheric observations contain contributions from known molecular emissions, we can use a synthetic spectrum of these emissions to simulate the reference spectrum.

The objective of hyperspectral analysis performed on test data is to determine the algorithm's ability to distinguish mines from the natural background in a scene. Three different search algorithms were tested. The first

algorithm determines a unique scale factor by comparing the two spectra, one for test data and one for reference spectrum, and dividing the maximum points from each. In order to evaluate the accuracy of this technique, the scale factors for different atmospheric altitudes were compared with known molecular abandances. This technique can only be used in cases where the brightest feature of the data is due to a component of the reference spectrum. The second method is similar to the first one, but it does not require that the reference spectrum produce the brightest feature in the data. It does, however, require that at least one feature of the reference spectrum dominates the corresponding feature in the data. The third method determines the total area below the product of reference spectrum and test data. Unlike the two previous methods there are no limitations for the third method. A more detailed description of search algorithms is given below.

A. DESCRIPTION OF DATA

Before presenting the details of the search algorithms, it is helpful to examine the test data and reference spectrum.

1. Test Data

Spectra of atmospheric airglow were obtained from a March 1992 rocket flight of the NPS MUSTANG instrument. These spectra have been analyzed from 1900 $\mathring{A}$ to 3100 $\mathring{A}$, over an altitude range of 100 km to 320 km above earth's

surface [Ref. 11 : p.19]. Figures 3.1, 3.2, 3.3 show typical spectra for 100 km, 155 km and 215 km. The spectra contain averaged intensities (in $\frac{R}{\mathring{A}}$) as a function of wavelength (in $\mathring{A}$). Twenty three different altitudes, each with 512 elements (intensities), were used to simulate the test data.

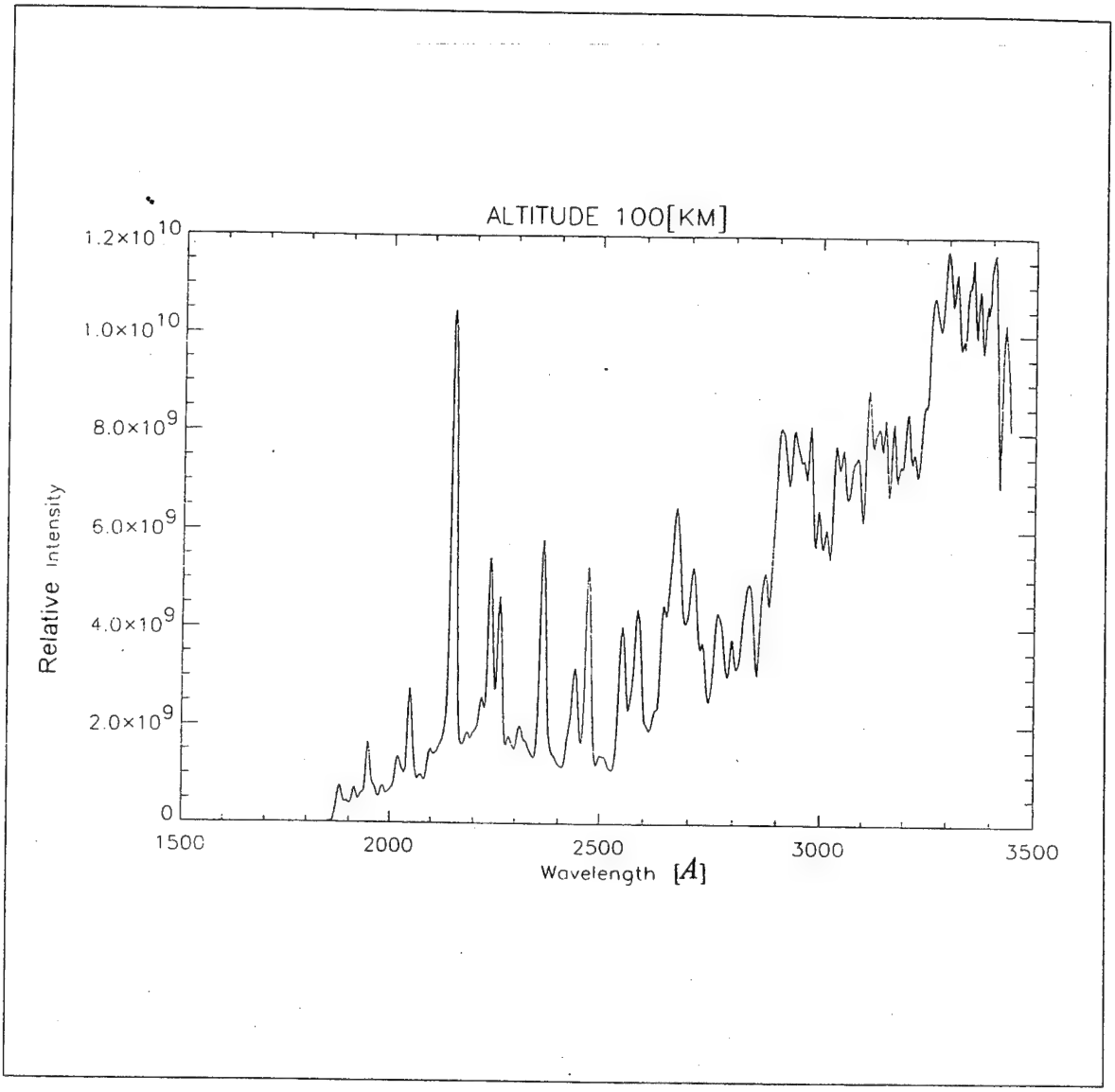

Figure 3.1: Data graph for an altitude of 100 km

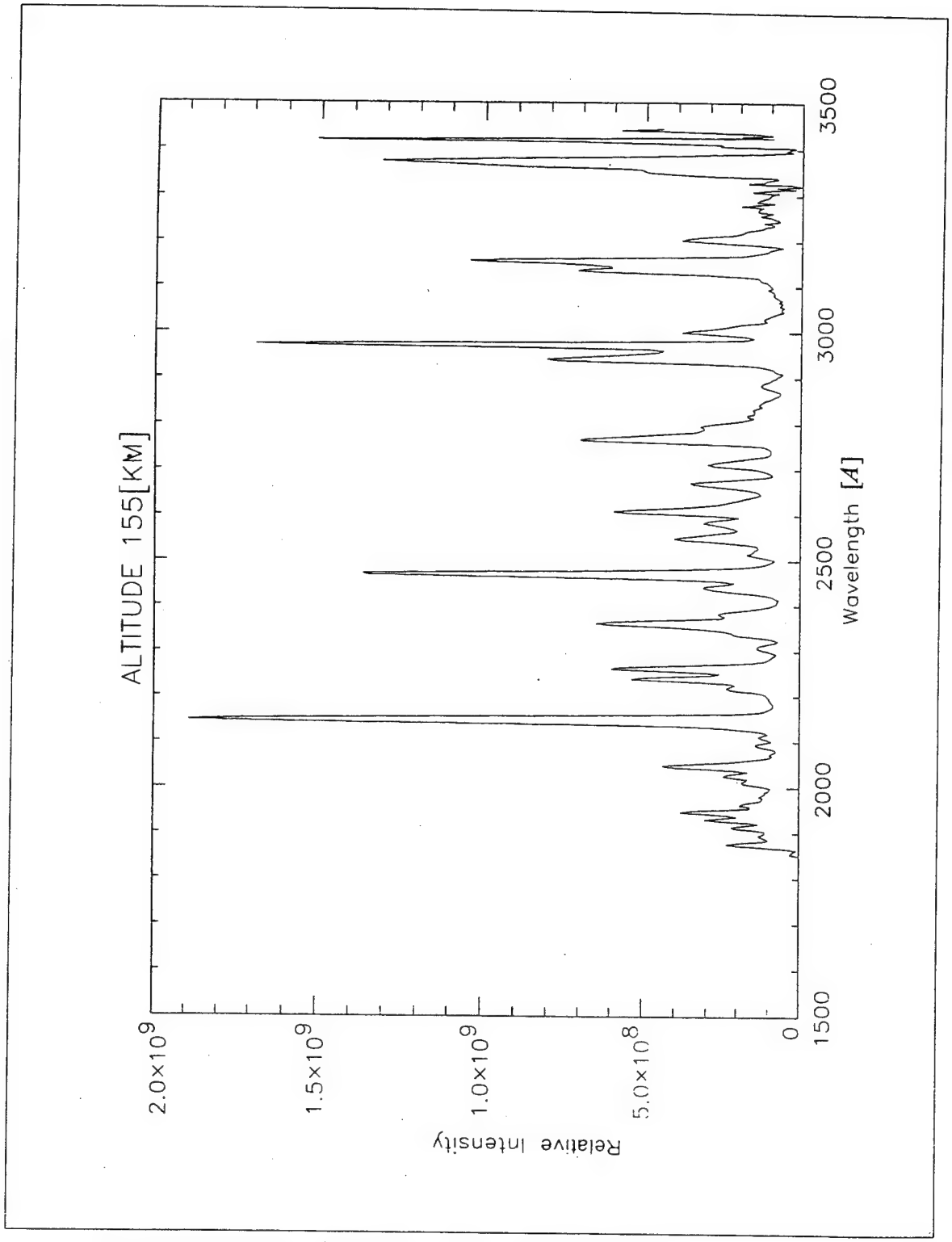

Figure 3.2: Data graph for an altitude of 155 km

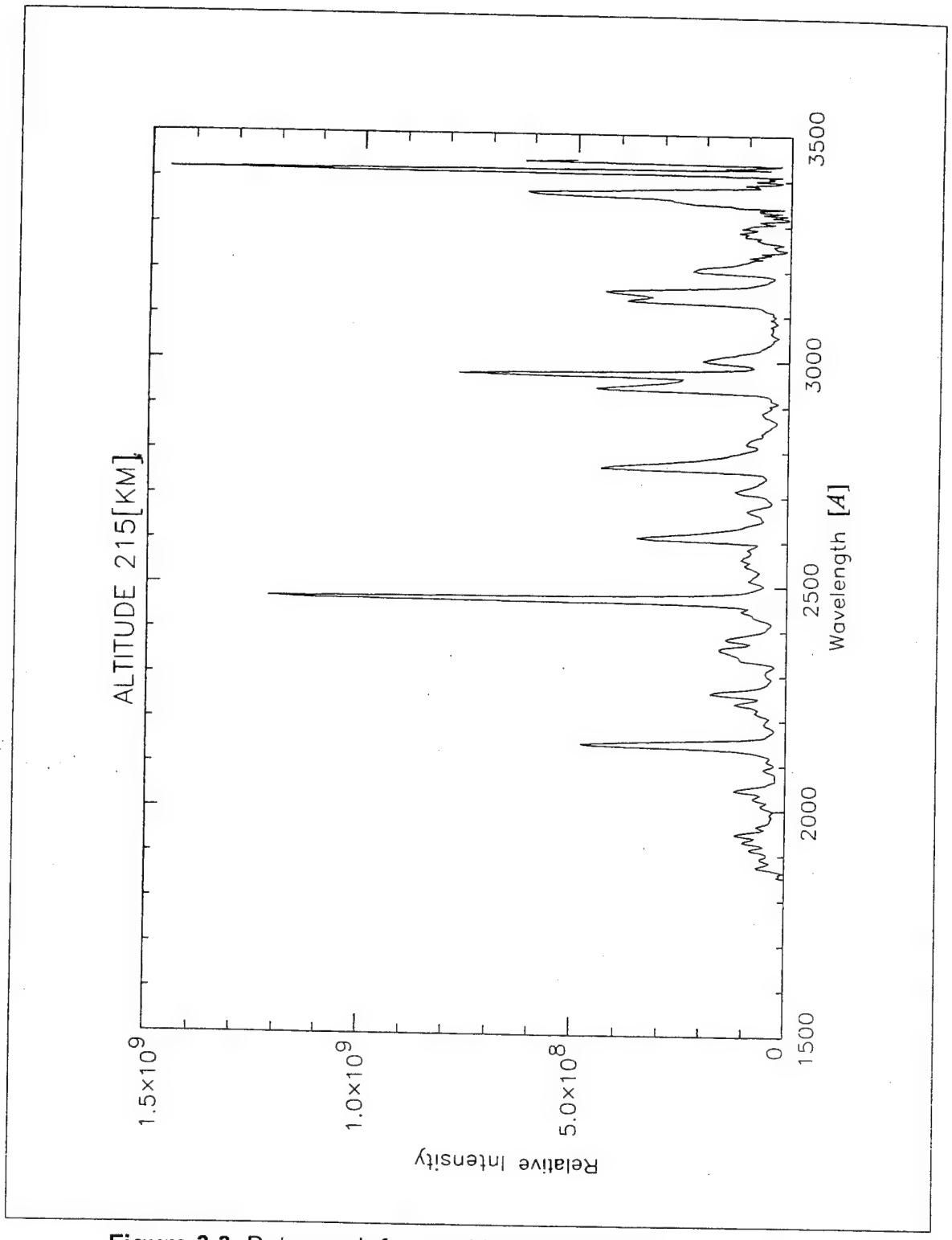

Figure 3.3: Data graph for an altitude of 215 km

2. Reference Spectrum

Computer-generated synthetic spectra written by Cleary [Ref. 11] were used for the generation of the Nitric Oxide (NO) γ-band emissions. Figure 3.4 shows a typical spectrum of the Nitric Oxide (1,3), (0,2), (1,4), (0,3), (1,5), (0,4) γ-resonance band emissions.

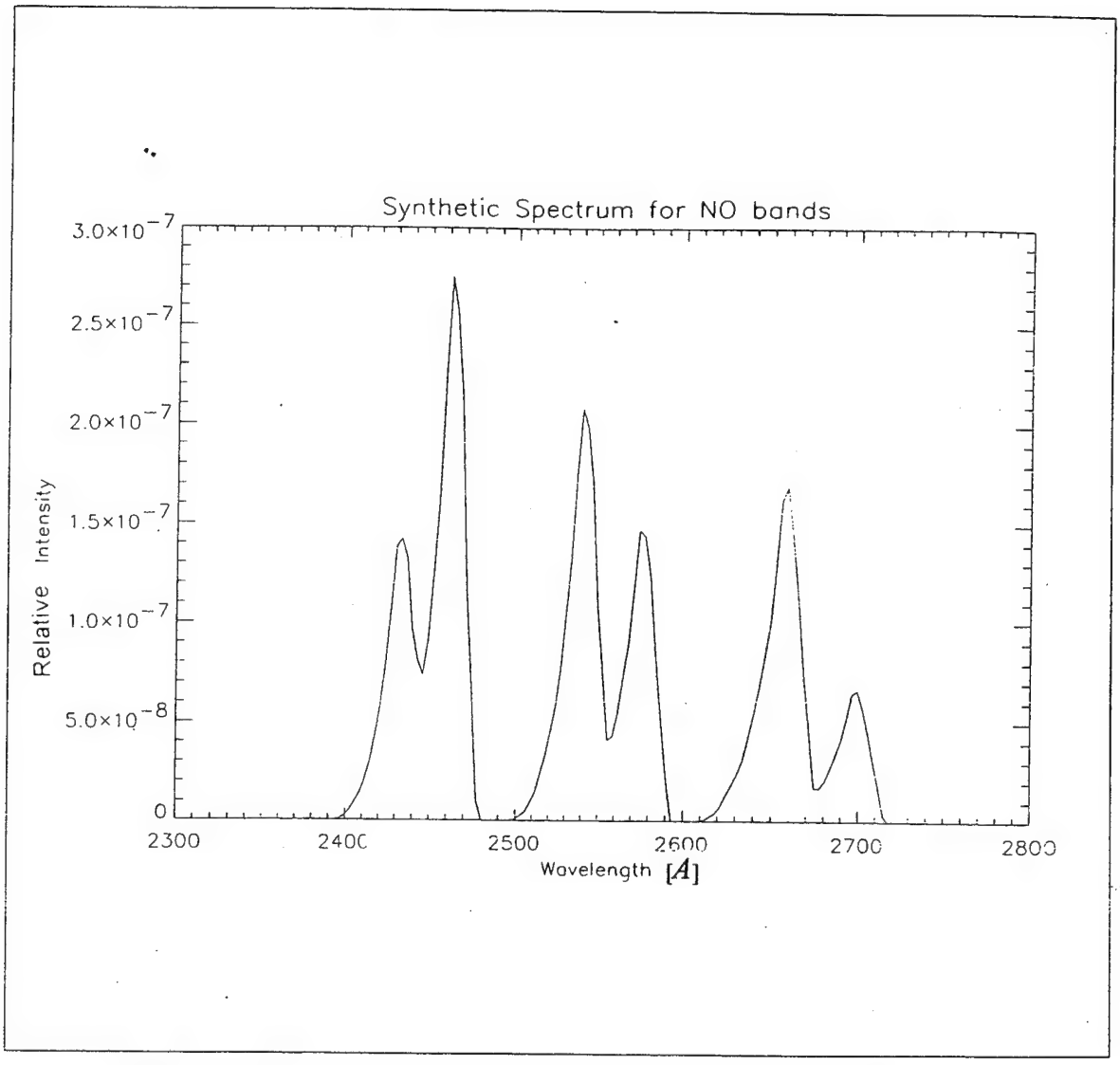

Figure 3.4: Synthetic data (reference spectrum) for NO

B. ALGORITHM TECHNIQUES

All of the computer code used in this study was written in Interactive Data Language (IDL®), version 4.0, designed by Research Systems, Inc. Details of the specific algorithms are given below.

1. Method of the local maxima

This method produces a scale factor that when multiplied by the reference spectrum produces a best fit to the observed data. The search algorithm first determines the maximum of the reference spectrum. Then, for every spectrum of the test data it calculates a unique scale factor by dividing the corresponding point of the data by the corresponding maximum point of the reference spectrum. Thus, every scale factor is generated using two maximum points:

- Reference spectrum maximum point
- Data's corresponding point

For the purposes of visual inspection, the reference spectrum is multiplied by the associated scale factor and compared with the corresponding spectrum of the test data. This provides an easy means to check the accuracy and reliability of the method. Figures 3.5 and 3.6, show the results for two different altitudes for the wavelength range 1900-2300 $\mathring{A}$, using this method. The maximum intensity point for the test data is shown as an asterisk above the solid curve. A crosshair

symbol above the dushed curve (reference spectrum) represents the corresponding maximum intensity point. One can also observe visually the relation between the test data and reference spectrum and how the two spectra are similar. Notice that the reference spectrum is shifted somewhat to the left with respect to test data curve. One would expect the reference spectrum to be centered under the test data. This discrepancy is thought to be the result of an uncertainty in the wavelength calibration of the MUSTANG instrument [Ref. 12]. Figure 3.7 shows a comparison of NO densities produced by this method with densities determined by others [Ref.10:p.53]. This method produces reasonable agreement at all altitudes.

It should be pointed out that this technique can only be used in cases where the brightest feature of the data is due to a component of the reference spectrum. Such is the case for the spectral feature at 2150 $\mathring{A}$ shown in Figures 3.5 and 3.6. It is often necessary to restrict the spectral range of the test data in order to satisfy this requirement. In Figures 3.5 and 3.6 the spectral range was restricted to 1900 and 2300 $\mathring{A}$ for this reason. Because the choice of this restricted spectral range involves a decision on the part of the operator, a more robust method was sought.

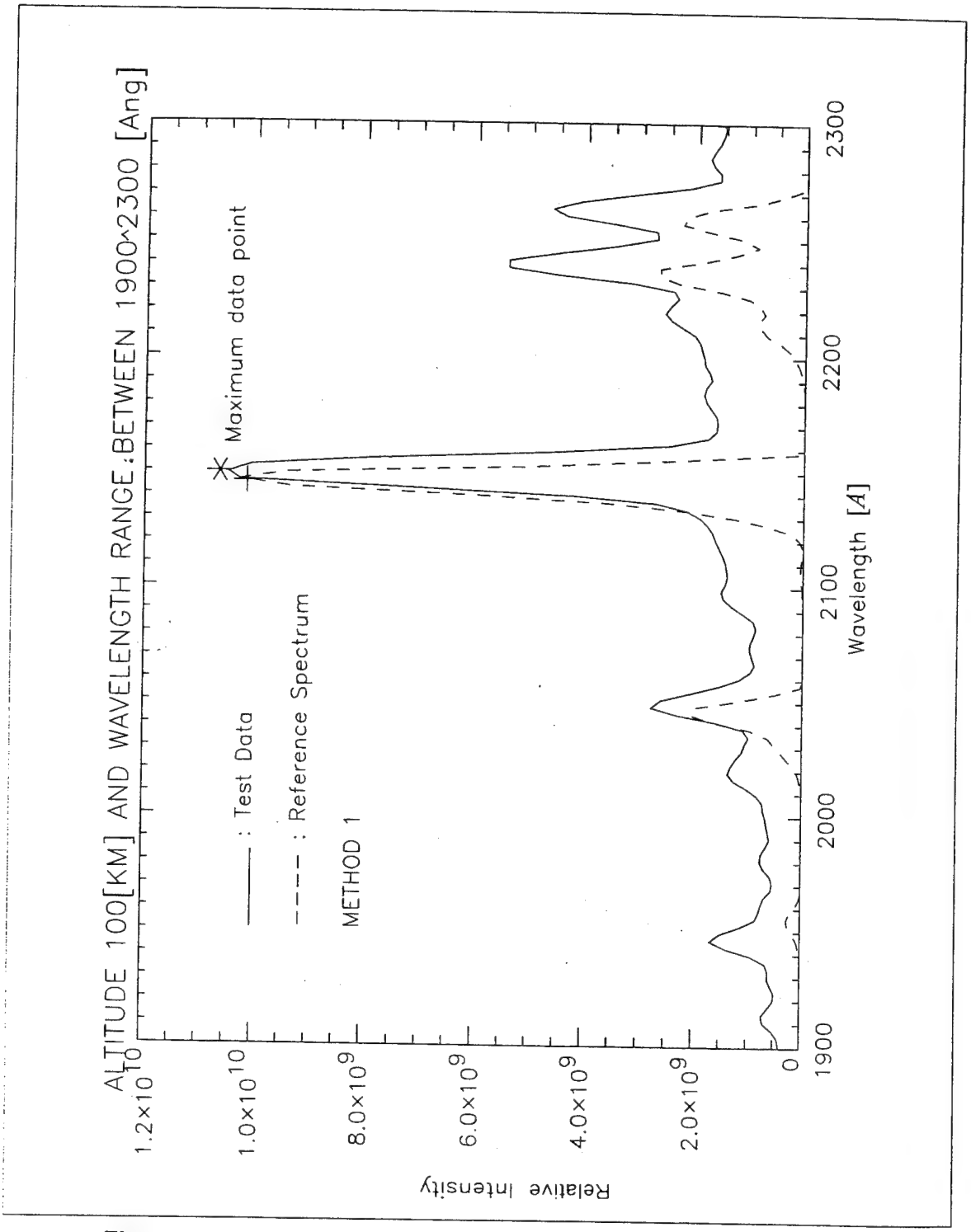

Figure 3.5: Data and fitted theory for an altitude of 100 km (Local Maxima method)

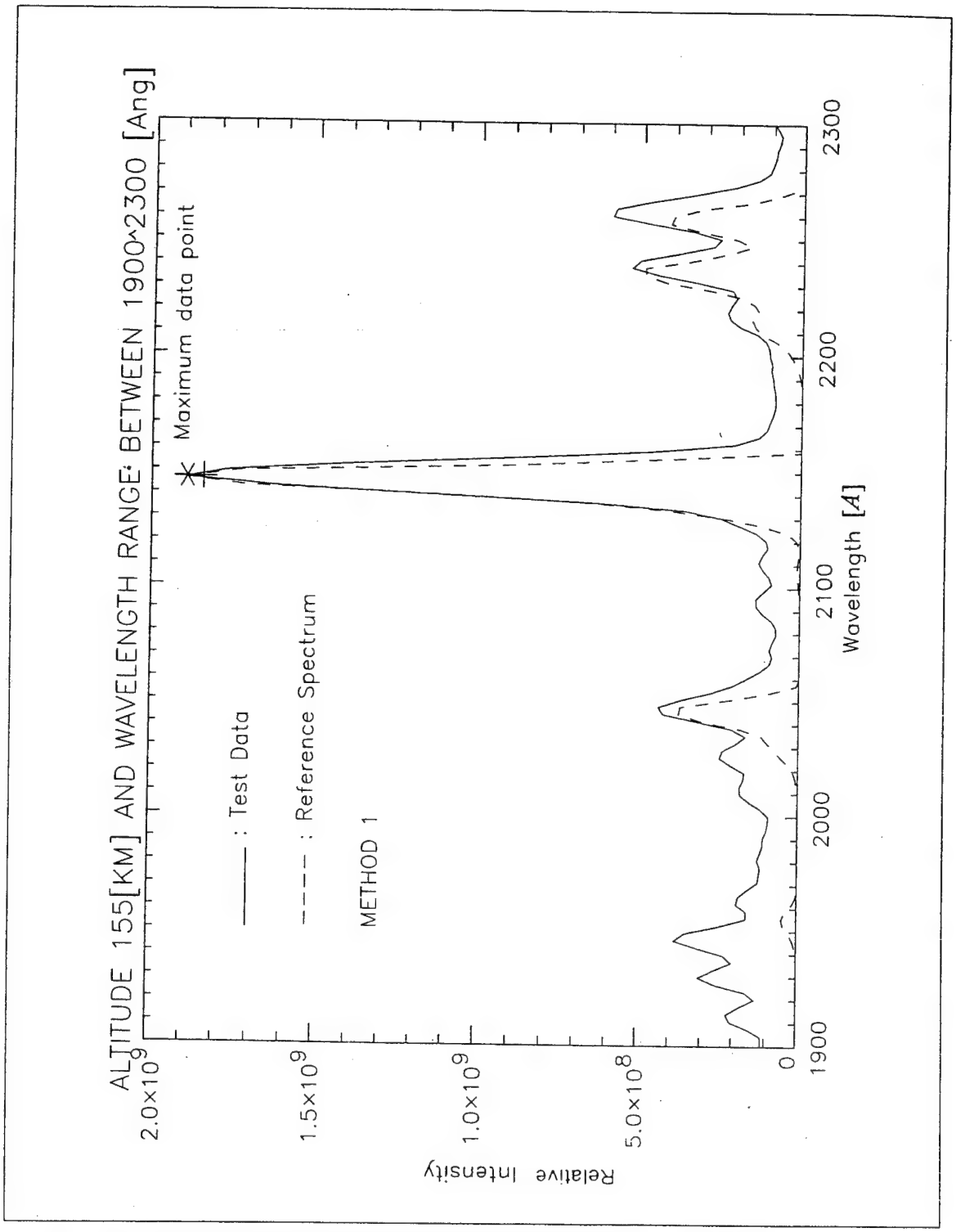

Figure 3.6: Data and fitted theory for an altitude of 155 km (Local Maxima method)

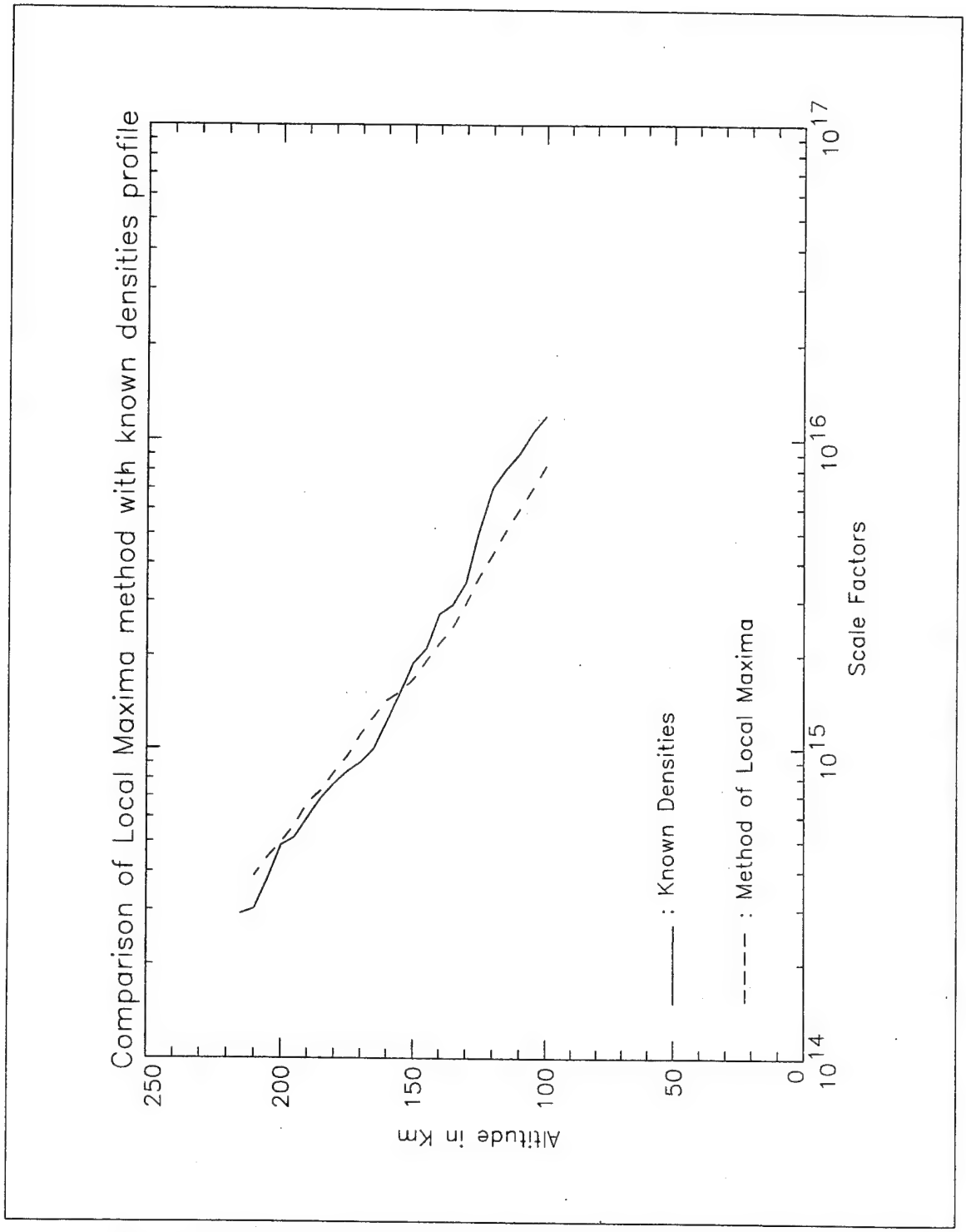

Figure 3.7: Comparison of Local Maxima method with known densities [Ref. 10 : p. 53]

2. Method of the Minimum Ratio

This method is similar to the method of Local Maxima in that the result is a scale factor that when multiplied by the reference spectrum, produces a best fit to the observed data. It differs from the previous method in that the full wavelength range of the data can be used. Thus, there is no need for a decision on the part of the operator prior to data analysis.

For this method, an array of scale factors is generated by taking the ratio of every element in the test data with the corresponding element of the reference spectrum. The minimum of this array is taken to be the overall scale factor for the given test spectrum. The reason the minimum is used for the overall scale factor can be understood as follows. Each ratio in the array can be thought of as the scale factor required to match a point in the reference spectrum with the data. The smallest scale factor will guarantee that the reference spectrum does not overestimate the data at any point in the spectrum. A total of twenty three scale factors is calculated after the completion of the algorithm.

In the development of the second method, several problems were faced. One of the most common was the "divide-by-zero" computer error. Because some values of the reference spectrum were very small, the ratio between test data and reference spectrum became a divide-by-zero error. This problem was solved by ensuring that every element in the reference spectrum was greater

than a certain minimum threshold. With a suitable choice for the threshold one could avoid divide-by-zero errors without affecting the final scale factor.

Figures 3.8 and 3.9, show the results for two different altitudes for the wavelength range 2400 to 2800 $\mathring{A}$, using the Minimum Ratio method. The local maximum intensity point for the test data is shown as an asterisk above the solid curve. A crosshair symbol above the dashed curve (reference spectrum) represents the corresponding maximum intensity point. Also, below the label "Threshold" we can see the suitable choice of the threshold (dashed line) that eliminates the divide-by-zero errors. One can also observe visually the relation between the test data and reference spectrum and how the two spectra are similar. Figure 3.10 shows a comparison of densities produced from this method with the known densities. Although not as good as Method 1, the densities shown in Figure 3.10 are still reasonable at all altitudes.

While this method does not require that the brightest feature be due to the reference spectrum (as in Local Maxima method), it does require that some spectral feature be primarily due to the reference spectrum. This is satisfied, for example, by the 2550 $\mathring{A}$ feature in Figure 3.9. In an attempt to remove this limitation, a new technique was sought.

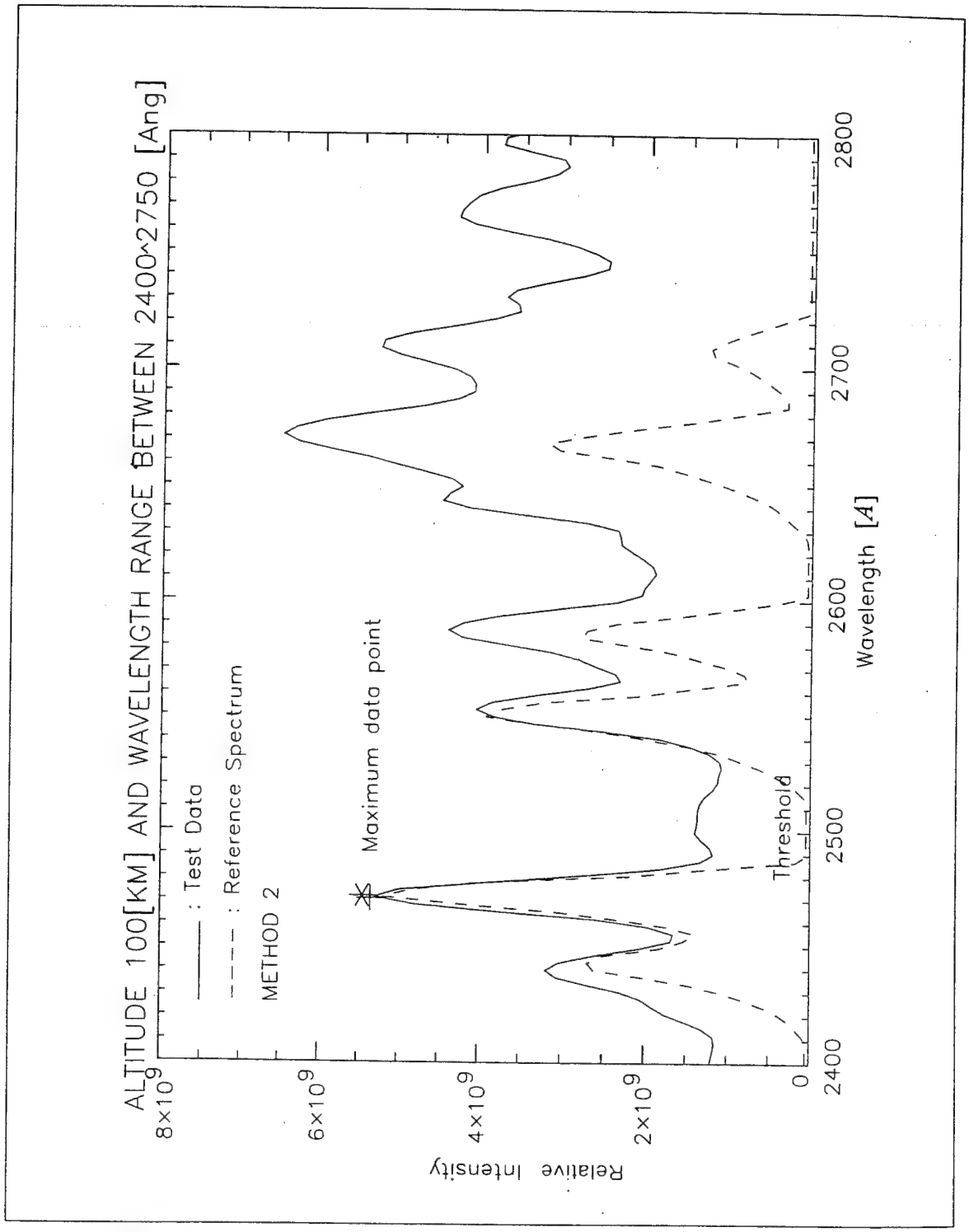

Figure 3.8: Data and fitted theory for an altitude of 100 km
(Minimum Ratio method)

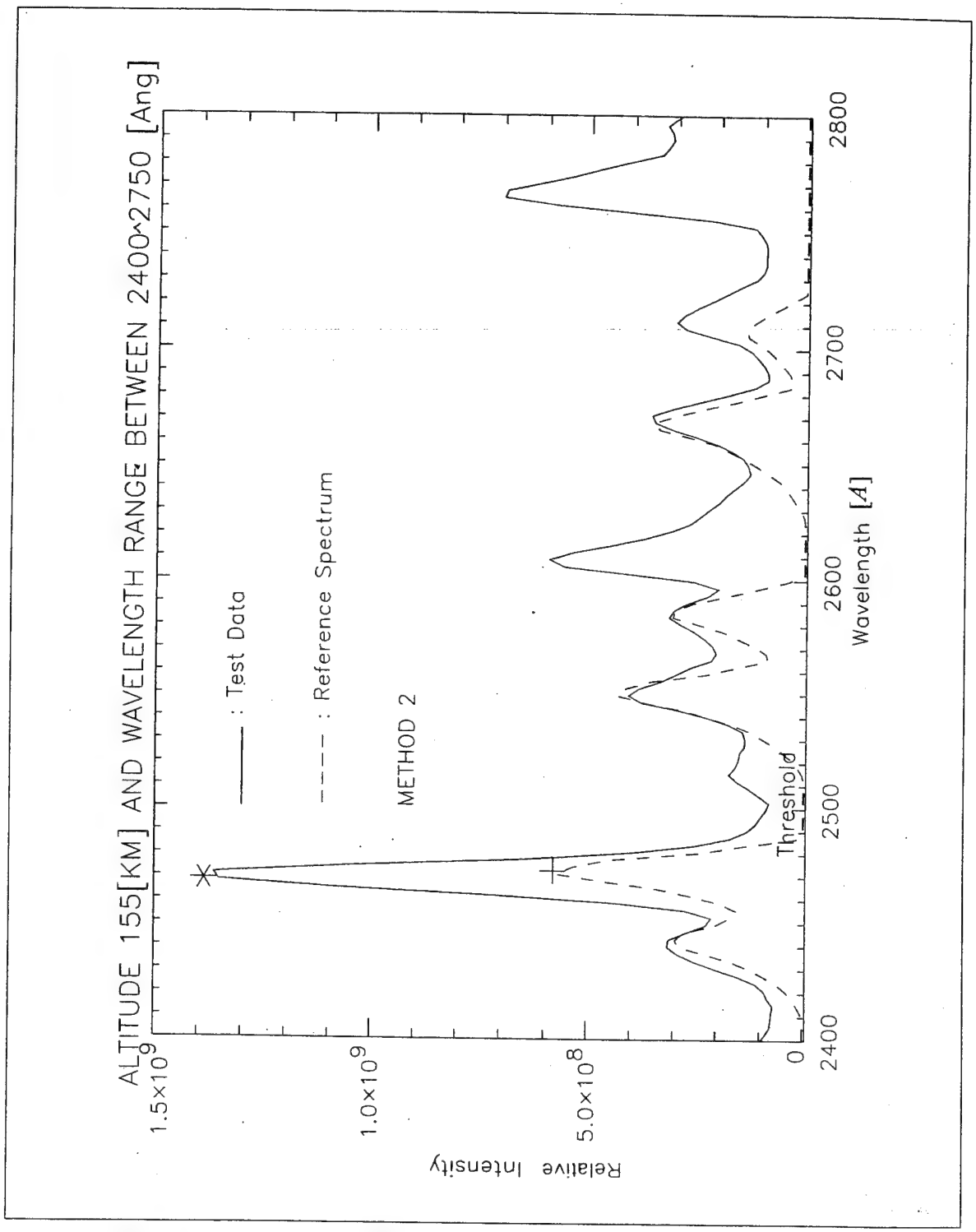

Figure 3.9: Data and fitted theory for an altitude of 155 km (Minimum Ratio method)

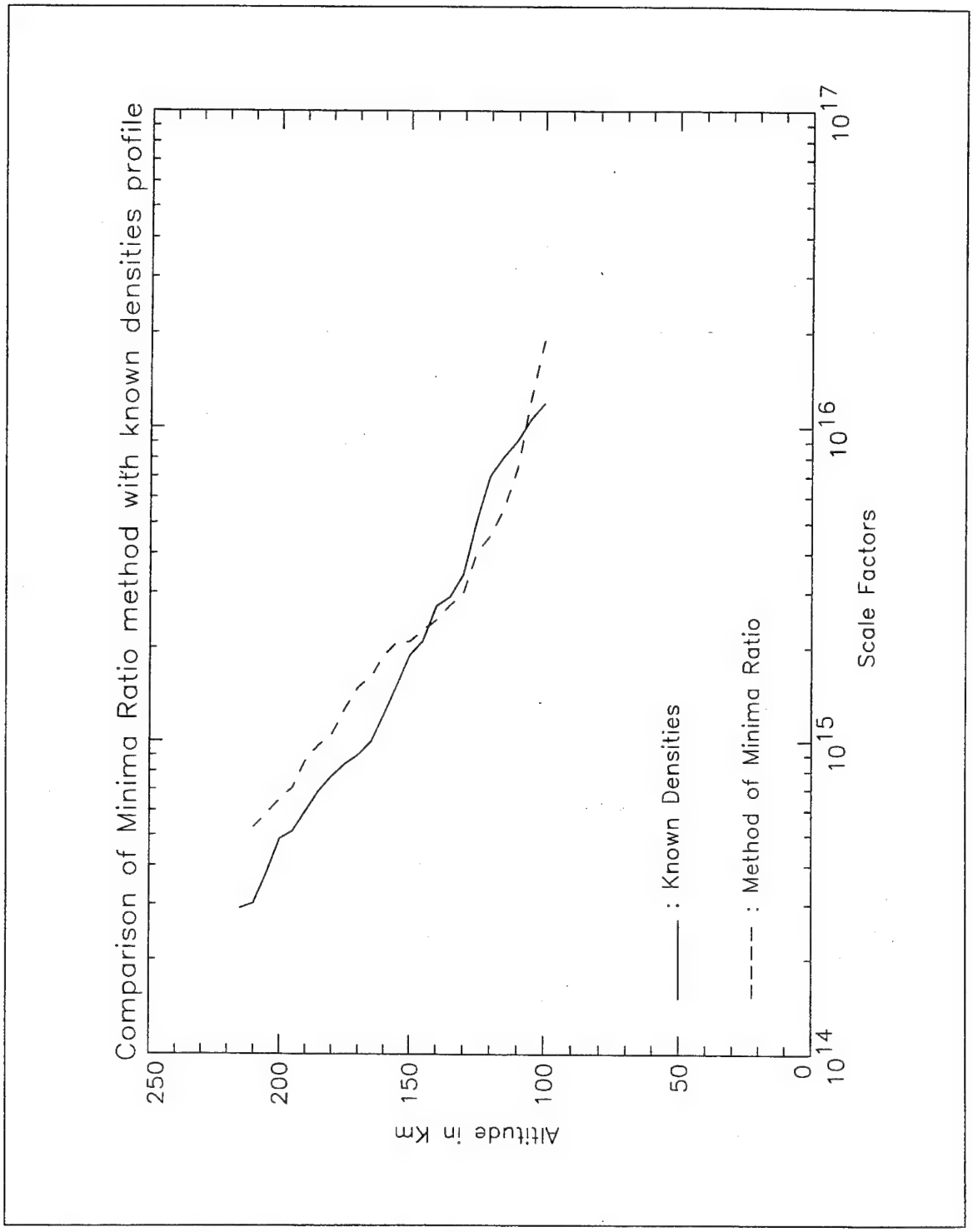

Figure 3.10: Comparison of Ratio Minima method with known densities [Ref. 10 : p. 53]

3. Method of the Total Area

Unlike the previous two methods, this method does not produce an absolute scale factor that is equal to a physical quantity. This method, instead, produces a relative scale factor that is proportional to the probability of detecting the target. The search algorithm multiplies the reference spectrum by the test data. The area of the resulting curve is calculated, and is assigned to a so-called "key-number".

The key-numbers obtained from different altitudes were multiplied by a fixed constant and compared with the known NO densities [Ref. 10 : p.53] , as is shown in Figure 3.11. The fixed constant was arbitrarily chosen to match the data. As a result, one should evaluate the accuracy of this method on the basis of the similarity in the shapes of the two curves not on the similarity in their magnitudes.

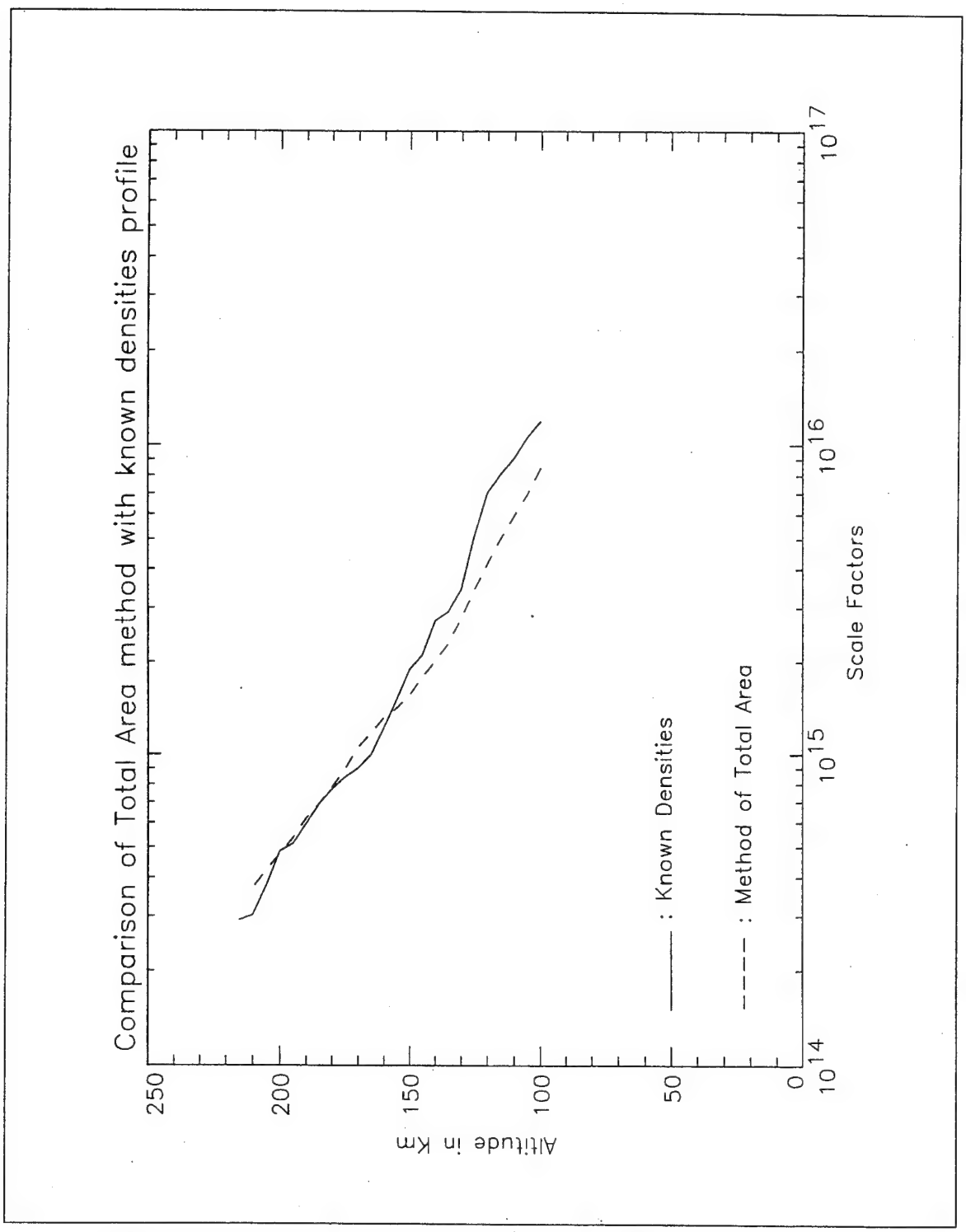

Figure 3.11: Comparison of Total Area method with known densities [Ref. 10 : p. 53]

IV. CONCLUSIONS AND RECOMMENDATIONS

The analysis of the search algorithms shows that the potential exists to use these methods in military applications. The ability to identify features in an image based solely on their spectral signature provides a new dimension to imagery interpretation. This chapter discusses the conclusions drawn as a result of the analysis performed on three search algorithms. Also, recommendations for proceeding with future efforts in these algorithms development are addressed.

A. SUMMARY OF FINDINGS

After hyperspectral analysis of the test and synthetic data, it is determined that the ability to distinguish simulated mine targets from the background features within a scene by comparing spectra, validates the concept of the used search algorithms. Also, of the three methods, the Total Area technique is preferred.

Hyperspectral analysis of the data using all three search algorithms is limited by two different constraints. The first is the signal-to-noise level of the reference spectrum that we have neglected. When noise is added to the spectrum, the performance of the search algorithms is expected to degrade.

The other limitation on the ability to derive information about mine targets within a scene using hyperspectral analysis is the wavelength range of the

sensor. One must decide which wavelength range contains the most unique features of a mine. For example, Figure 4.1 shows a comparison of the spectrum of a Mk-TM46 antitank mine with the spectrum of beach sand. Both spectra were obtained in the laboratory. For this wavelength range there is little difference between the two spectra. Obviously a different wavelength range is needed. The presence of unique spectral features would allow the isolation of a particular target (mine).

Figure 4.2 shows an overall comparison of the three search algorithms with a profile of known densities [Ref. 10 : p.53]. All three produce reasonable fits. The main difference between these algorithms is in their applicability. Method 1 requires the brightest reference spectrum while Method 3 can handle the weakest.

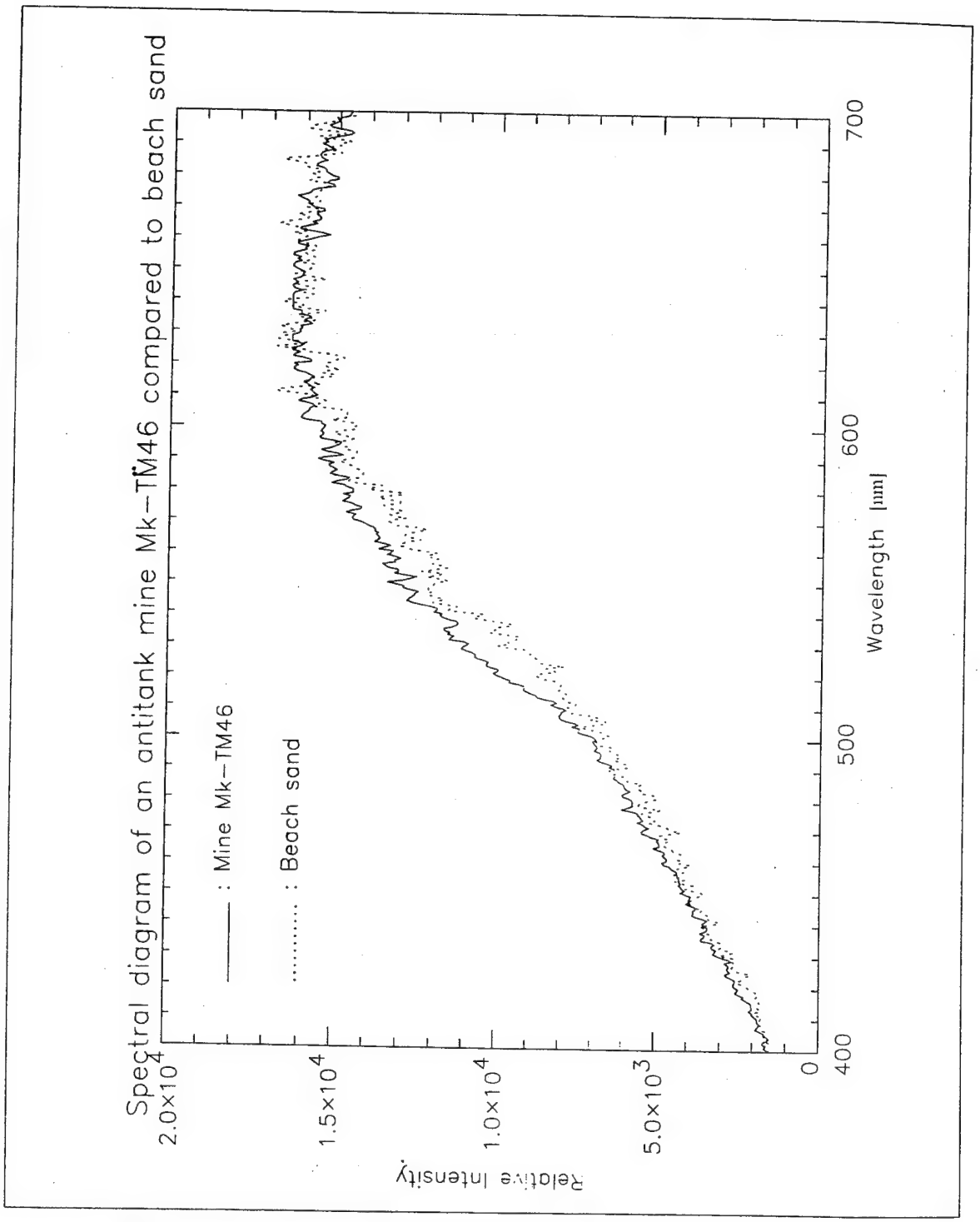

Figure 4.1: Spectral diagram of an antitank mine Mk-TM46 compared to spectrum of beach sand

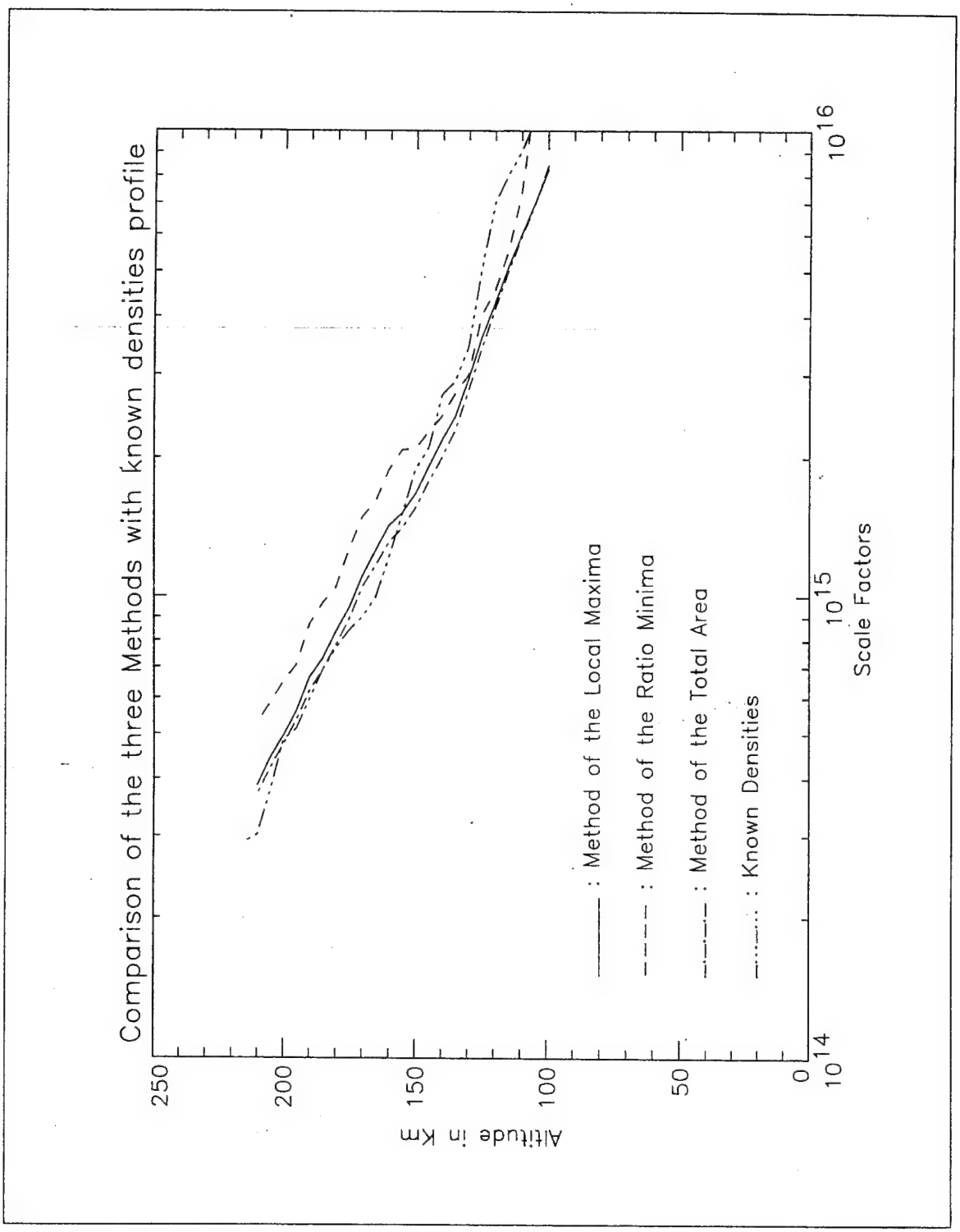

Figure 4.2: Comparison of the three methods with known densities profile [Ref. 10 : p.53]

B. RECOMMENTATIONS AND FUTURE WORK

The military should pursue development of hyperspectral imagery to enhance current mine detection capabilities. An airborne trial of this study will show the effectiveness and possible algorithm conflicts of all three methods. The proposed system for the airborne experiment can include a spectrometer apparatus on board a UAV (unmanned-air- vehicle). The UAV can be launched and recovered from any sea or land-based platform having remote control capabilities and a HF (high frequency) transmitter that will send back the measurements to a computer system.

There is more work to be done in the development of search algorithms. First and foremost, the capability of dealing with noisy data must be addressed. Second, a determination of the most appropriate wavelength range for a given target must be made. Both problems were neglected in this study since ideal (without noise) data files and preselected wavelength ranges were used by the search algorithms.

The experiment to test the prototype system, as mentioned above, should validate the detection concept of hyperspectral technology. A future experiment would also help identify any deficiencies in the current algorithms.

APPENDIX - COMPUTER PROGRAMS/LISTINGS

A variety of routines were written for use in the IDL language to manipulate the data. A complete annotated listing is provided for each program used.

A. SUMMARY OF PROGRAMS UTILIZED IN DATA/THEORY MANIPULATION

Each of the major programs used in analyzing the mine's detection method is described below.

1. METHOD1.PRO

This program performed the data and theory manipulation and calculations using the method of Local Maxima. The two input files contain all the data information in asci (*.asc) and binary format (*.dat). Actually the binary format file was the product of a subroutine program (see later CONVERSION.PRO) that performs conversion between asc-files and dat-files. It is preferable and more handy to deal with dat-files instead asc-files. The reference spectrum was calculated using a subroutine. A for-loop was used to calculate all the scale factors for every altitude stored in a separate output file, as an array of twenty three ellements. Inside the loop the ratio of the maximum data point over maximum theory point was taken to provide the right scale factors.

2. METHOD2.PRO

This program performed the data and theory manipulation and calculations using the minima ratio method. The same subroutines were used, as mentioned above, for data and theory. An additional line was provided to fix divide-by-zero errors for reference spectrum. The point-by-point ratio was put inside a for-loop, and the scale factors were produced by taking the minimum of the ratio, then stored in an output file as an array of twenty three ellements for further usage.

3. METHOD3.PRO

This program performed the data and theory manipulation and calculations using the method of the total area. A for-loop is used to determine the corresponding test data key-numbers.

4. CONVERSION.PRO

This program performed all the necessary file conversions between asci (*.asc) and binary format (*.dat). These conversions are important because they simplify the way handling of file information by the computer algorithm.

B. LISTINGS OF IDL PROGRAMS USED IN DATA MANIPULATION

The following subsections give complete listings of the main IDL programs used in this study.

1. METHOD1.PRO Program listing

```
**********************************METHOD1.PRO**************************************
;  Modified 15 Ian 96 by Dimitrios Nikolaidis.
;  This program calculates the desired scale factors using the method
;  of local maxima.
@~mustang/syn/gamsyn
openr, 1 , '~mustang/m92/m92up_int.dat'
a = assoc ( 1, fltarr(512) )
wl = a ( 0 )            ;  The wavelength
openr, 2 ,   '~mustang/m92/m92up_int.asc'
readf, 2 , npts , nrecs
t = 1500                ;  The temperature
intg = wl * 0
gamsyn , t , 1 , 0 , wl , intg
gamsyn , t , 2 , 0 , wl , intg
gamsyn , t , 3 , 0 , wl , intg
gamsyn , t , 2 , 2 , wl , intg
gamsyn , t , 1 , 1 , wl , intg
gamsyn , t , 0 , 0 , wl , intg
gamsyn , t , 3 , 1 , wl , intg
gamsyn , t , 3 , 2 , wl , intg
```

```
intg = smooth ( intg , 3 )
gammamax = max ( intg )          ;  The maximum point of the reference
                                 ;  data.
maxpixel = !c
fac_1 = fltarr ( nrecs-1 )
openw , 3 , 'thesis/file_factors_1.dat' , 4 * npts
ff_1 = assoc ( 3 , fltarr ( nrecs ) )
for  j = 0 , ( nrecs-20 ) do begin
    data = a ( j + 1 ) * 3.13E6
    datamax = max ( data ( maxpixel ) )    ;  The maximum point of the
                                           ;  test data.
    fac_1 ( j ) = datamax / gammamax       ;  The scale factors array.
endfor
ff_1 ( 3 ) = fac_1
end
```

2. METHOD2.PRO Program listing

```
**********************************METHOD2.PRO**************************************
;  Modified 15 Feb 96 by Dimitrios Nikolaidis.
;  This program calculates the desired scale factors using the ratio
;  minima method.
```

```
@~mustang/syn/gamsyn

openr, 1 , '~mustang/m92/m92up_int.dat'

a = assoc ( 1, fltarr(512) )

wl = a ( 0 )          ;  The wavelength

openr, 2 ,  '~mustang/m92/m92up_int.asc'

readf, 2 , npts , nrecs

t = 1500              ;  The temperature

intg = wl * 0

gamsyn , t , 1 , 3 , wl , intg

gamsyn , t , 0 , 2 , wl , intg

gamsyn , t , 1 , 4 , wl , intg

gamsyn , t , 0 , 3 , wl , intg

gamsyn , t , 1 , 5 , wl , intg

gamsyn , t , 0 , 4 , wl , intg

intg = smooth ( intg , 3 )

theory_2 = shift ( intg , 3 )

theory_2 = theory_2 > ( max ( theory_2 ) / 100. )

fac_2 = fltarr ( nrecs-1 )

openw , 4 , 'thesis/file_factors_2.dat' , 4 * npts

ff_2 = assoc ( 4 , fltarr ( nrecs ) )

for  i = 0 , ( nrecs-2 ) do begin
```

```
    data = a ( i + 1 ) * 3.13E6
    ratio = 1.1 * data ( 189 : 285 ) / theory_2 ( 189 : 285 )
    fac_2 ( i ) = min ( ratio )          ;  The scale factors array.
endfor
ff_2 ( 4 ) = fac_2
close , 1 , 2
end
```

3. METHOD3.PRO Program listing

```
**********************************METHOD3.PRO**************************************
;  Modified 15 Mar 96 by Dimitrios Nikolaidis.
;  This program calculates the desired key-numbers using the method
;  of totall area.
@~mustang/syn/gamsyn
openr, 1 , '~mustang/m92/m92up_int.dat'
a = assoc ( 1, fltarr(512) )
wl = a ( 0 )          ;  The wavelength
openr, 2 ,  '~mustang/m92/m92up_int.asc'
readf, 2 , npts , nrecs
t = 1500              ;  The temperature
intg = wl * 0
```

```
gamsyn , t , 1 , 0 , wl , intg

gamsyn , t , 2 , 0 , wl , intg

gamsyn , t , 3 , 0 , wl , intg

gamsyn , t , 2 , 2 , wl , intg

gamsyn , t , 1 , 1 , wl , intg

gamsyn , t , 0 , 0 , wl , intg

gamsyn , t , 3 , 1 , wl , intg

gamsyn , t , 3 , 2 , wl , intg

intg = smooth ( intg , 3 )

key_numb = fltarr ( 23 )

for  i = 0 , 22  do begin

    key_numb ( i ) = total ( intg * a ( i + 1 ) * 3.13E6 )  ; The key-numbers

endfor

end
```

4. CONVERSION.PRO Program listing

```
**********CONVERSION.PRO**********

PRO conv , file , nrecs

openr , 2 , '~mustang/m92/ ' + file + ' .asc '

readf , 2 , npts , nrecs

openw , 1 , '~mustang/m92/ ' + file + ' .dat ' , 4 * npts

a = assoc ( 1 , fltarr ( npts ) )
```

```
dat = fltarr ( npts )
for  j = 0 , ( nrecs - 1 ) do begin
     readf , 2 , dat
     a ( j ) = dat
endfor
close , / all
end
```

LIST OF REFERENCES

1. *Ammunition (Including grenades & mines),* KJW Goad & DHJ Halsey, Royal Military College of Science, Shrivenham, UK, 1982.

2. *Manual of Remote Sensing,* 2nd ed., v.1, American Society of Photogrammetry, 1983.

3. Halliday, D., and Resnick, R., *Fundamentals of physics,* 3rd ed., John Wiley & Sons, Inc., 1988.

4. *Optics,* by Miles V. Klein and Thomas E. Furtak, 2nd ed., John Wiley & Sons, Inc., 1986.

5. Slater, P. N., *Remote Sensing Optics and Optical Systems,* Addison-Wesley Publishing Company, Inc., 1980.

6. *Introduction to airborne radar,* G. S. Gill, G. W. Stimson, HUGHES Aircraft Company, 1983.

7. Egan, W. G., *Photometry and Polarization in Remote Sensing,* Elsevier Science Publishing Company, Inc., 1985.

8. *Class notes.*

9. Swain, P. H., *Remote Sensing,* McGraw-Hill, Inc.,1978.

10. Marron, Antony C., *An Analysis of Ionospheric Dayglow from Observations of the Naval Postgraduate School Middle Ultraviolet Spectrograph (MUSTANG),* Master's Thesis, Naval Postgraduate School, Monterey, California, December 1993.

11. Cleary, D. D., *"Daytime High-Latitude Rocket Observations of the NO γ, δ, Bands,"* Journal of Geophysical Research, v.91, 1986.

INITIAL DISTRIBUTION LIST

1. Defense Technical Information Center.....2
   8725 John J. Kingman Rd., STE 0944
   Ft. Belvoir, VA 22060-6218

2. Dudley Knox Library.....2
   Naval Postgraduate School
   411 Dyer Rd.
   Monterey, California 93943-5101

3. Dr. William B. Colson.....1
   Physics Department, Chairman PH
   Naval Postgraduate School
   Monterey, California 93943-5000

4. Dr. D. D. Cleary.....3
   Physics Department, PH/Cl
   Naval Postgraduate School
   Monterey, California 93943-5000

5. Dr. Suntharalingam Gnanalingam.....1
   Physics Department, PH/Gm
   Naval Postgraduate School
   Monterey, California 93943-5000

6. Dr. Xiaoping Yun.....1
   Department of ECE, EC/Yx
   Naval Postgraduate School
   Monterey, California 93943-5000

7. LT Dimitrios Nikolaidis.....2
   Vas. Alexandrou 21
   Moschato, 18344
   Athens, Hellas (Greece)